Experimental Determination of the Spatial Sensitivity of a ^{3}He Neutron Spectrometer for Field Analog Experiments to Reunite Planetary Science and Terrestrial Hydrology

by

Nicole Gonzales

A Thesis Presented in Partial Fulfillment
of the Requirements for the Degree
Master of Science

Approved October 2024 by the
Graduate Supervisory Committee:

Craig Hardgrove, Chair
Mark Robinson
Edward Garnero

ARIZONA STATE UNIVERSITY

December 2024

ABSTRACT

Neutron Spectroscopy is a non-invasive way to estimate the hydrogen content (reported as 'Water-Equivalent-Hydrogen' or WEH, an indirect measurement of H_2O) of the top 1 m of the soil. Terrestrial hydrologists use passive neutron spectroscopy (PNS) to estimate soil moisture (water found between the grains) over time. Utilizing stationary instruments enables changes in the neutron count rates to be used as a proxy for changes in soil moisture caused by fluctuations in groundwater, precipitation, and vegetation, while soil and rock composition remain constant. Planetary science missions use PNS to analyze the WEH at points along a traverse via a mobile platform on rocky worlds with thin atmospheres without precipitation and vegetation. Detected changes in neutron counts on mobile platforms are the result of geochemistry.

Herein, a new, portable PNS instrument, referred to as 'rovers' (RVs), is utilized to experimentally characterize the radial sensitivity (footprint), orientation and vegetation sensitivities, and moderator thickness, to characterize the differences between moderated and bare detectors.

PNS instruments measure neutron counts from moderated and bare neutron detectors, each sensitive to different energy ranges and used (together) as a proxy for variations in abundances of neutron absorbing and neutron scattering elements. Terrestrial hydrologists implement a method to remove counts from neutrons emitted and moderated in the atmosphere to calculate ground WEH from the moderated detector, but they note that the bare detector likely has a smaller footprint and needs additional characterization.

Changing the environmental factors within the radial sensitivity (by removing vegetation, or increasing the distance from a body of moderators), determines how each factor affects the count rates.

Experimentation in the field: provided maximum radial sensitivities for the new, smaller, portable moderated and bare detectors (31 m and 2 m, respectively), which increases further from the surface or in the vertical orientation; determined adjustments are needed for vegetation (~10% increase in epithermal, and ~15% decrease in thermal counts); and increased portability (removing a layer of moderator).

ACKNOWLEDGMENTS

Special thanks to my advisor Craig Hardgrove and his family as well as the Hardgrove Planetary Nuclear Science Team at ASU for their continued support, encouragement, patience, field support, and insightful foundational knowledge that was always there to help guide me while considering neutron spectrometers on Earth, Mars, Mercury, Venus, and the Moon! I could not have done this without all of you!

Additional thanks to the NASA Lunar Reconnaissance Orbiter project for providing funding.

And a special thanks to Ed Garnero for his unending support and patience and inspiring endless joy for his research and that of all scientists he finds himself working with!

We would also like to thank the Lake Pleasant Regional Park and the Jornada Basin LTER for providing access to their ecological resources for our field work.

We also extend our thanks to Dr. Trenton Franz at the University of Lincoln, Nebraska and Dr. Enrique Vivoni and his graduate student research team at ASU, for their correspondence, COSMOS and LTER access, and guidance that allowed us to gain an understanding of the terrestrial hydrology instruments and methods.

Special thanks to fellow MS student and recent graduate Ruby Hurtado for being such a wonderful and patient field partner as we learned our way around terrestrial CRNS instruments and methods!

And last but not least, a special thanks to Hydroinnova and Quaesta Instruments for engineering our custom portable neutron spectrometer backpack instrument, without which this work would not have been possible!

TABLE OF CONTENTS

Page

LIST OF FIGURES vi

CHAPTER

1 INTRODUCTION 1

Significance and State of the Art 1

Goals and Objectives 3

Background 4

The Source of Neutrons for PNS 4

Neutron Lethargy Spectrum 5

Atmospheric Corrections 13

Calculating SM and WEH 16

Radial Sensitivity 19

2 MATERIALS, METHODS, AND RESULTS 23

Materials 23

Introduction to the Instruments 23

Proportional ^{3}He Detectors 23

COSMOS CRNS 28

RVs 29

Similarities and Differences of Terrestrial and Planetary CRNS 33

Orientation 33

Portability and Moderator Thickness 34

Thermal and Epithermal Detector Uses 35

CHAPTER Page

Topography....38
Methods and Results....38
Vegatation Sensitivity Test....38
Radial Sensitivity Scale and WEH Confirmation Test....43
Radial Sensitivity Quantification Test....52
Orientation Test....65
Moderator Thickness Test....68
3 CONCLUSIONS....75
Summary of Results....75
Earth....76
The RV Instruments....78
Moon and Mars Comparison....78
Moon Comparison....79
Mars Comparison....79
Mercury Comparison....80
Venus Comparison....80
Recommendations for Future Studies....83
REFERENCES....84

LIST OF FIGURES

Figure Page

1. Spallation Emitted Neutrons (modified from [Parsons, 2020]) 6
2. Neutron Lethargy Energy Spectrum in a Variety of Scenarios 8
3. Epithermal and Thermal Neutron Intensity Fluctuation as Measured Before and After Vegetation Removal from [Vather et al., 2020] 12
4. WEH Maps from Detectors in Orbit and On the Surface 19
5. WEH Comparison Between Planetary PNS and Terrestrial Hydrology PNS.....21
6. ^{3}He Proportional Counters and Neutron Energies 23
7. Neutron Energy Ranges and Detector Sensitivity Ranges 26
8. The Neutron Lethargy Spectrum Before and After Atmospheric Correction Factors are Applied to the Moderated (Epithermal) Data.....27
9. The Two PNS Instruments Used Herein: COSMOS and RVs 28
10. Polyethylene Moderator In the Moderated RV Detectors 30
11. Both RV Instruments and the COSMOS Instrument 31
12. The Various Configurations of the RV Instruments 32
13. Orientation Results From Peplowski et al., 2023 34
14. Vegetation Test Changes in Average Count Rate 40
15. Neutron Lethargy Fluctuations Before and After Tree Removal 42
16. Map of the Small Playa Site 44
17. Averages of Raw Data Stepping Incrementally Outwards at the Small Playa ..45
18. Corrected Neutron Count Rates Stepping Incrementally Outwards at the Small Playa 46

Figure Page

19. WEH for Each RV Station 46

20. Sample Map of the Small Playa Site 47

21. Sample-Measured WEH Compared to RV-Calculated WEH 49

22. Neutron Lethargy Spectra for Radial Sensitivity Order of Magnitude Test at the Small Playa 51

23. Maps of Fireman's Cove at Lake Pleasant 54

24. Lake Plesant Kayak Route and Data Collected 56

25. Data Collected at Fireman's Cove 58

26. Modifying the 86% Method for the Bare Detector 62

27. Incremental Neutron Lethargy Plots for Each Orientation at Fireman's Cove 63

28. Neutron Lethargy Spectra for the Small Playa (SP) Orientation Test 66

29. Map of the Moderator Thickness Test 69

30. The Raw Data From the Moderator Thickness Test 70

31. Average Raw Counts and Average WEH Calculations for Each Moderator Thickness 71

32. Neutron Lethargy Spectra Per Moderator Thickness 73

CHAPTER 1

INTRODUCTION

Significance and State of the Art

In several planetary neutron spectroscopy papers, it is stated that "Cosmic-ray protons do not reach Earth's surface, so an alternative means of generating planetary-like neutron spectra is required" [Peplowski et al., 2023], or otherwise explained as "some planetary bodies such as Venus, Titan and the Earth have atmospheres that are dense enough that the GCR [galactic cosmic ray] particles are absorbed before reaching the planetary surface" [Parsons, 2020]. However, terrestrial hydrologists do acknowledge that "at sea level, the neutron flux density is small and difficult to measure since it is easily perturbed by local terrain" [Hewitt et al., 1976], it is still utilized frequently to monitor soil water content, primarily in agricultural, forest, and desert watershed settings, and has been for decades [Brooks and Klein 2002; Hewitt et al., 1976; Andreasen et al., 2016, 2017; Franz et al., 2012, 2013, 2015, 2016, 2018; Hurtado et al., 2023, 2024; Schreiner-McGraw et al., 2016; Vather et al., 2018, 2020; Zreda et al., 2008, 2012; Bogena et al., 2013; Desilets et al., 2006, 2010, 2013, 2017; Kohli et al., 2015; Rosoleum et al., 2013; Schron et al., 2017, 2021, 2023; Goldhagen et al., 2002; Iwema et al., 2021; Rasche et al., 2023; Schattan et al., 2017; Weimar et al., 2020; Baatz et al., 2015]. Brooks and Klein summarized the history of neutron spectrometry and traced ^{3}He proportional counters (the same type of detectors used herein), back to 1960 [Brooks and Klein, 2002].

In fact, the debate in terrestrial hydrology is not whether PNS on Earth is possible, but simply what each of the two detectors is best suited to measure. While the moderated detector is well characterized [Andreasen et al., 2016, 2017; Franz et al., 2012, 2013,

2015, 2016, 2018; Hurtado et al., 2023, 2024; Schreiner-McGraw et al., 2016; Vather et al., 2018, 2020; Zreda et al., 2008, 2012; Baatz et al., 2015], many terrestrial hydrology papers concur with Andreasen et al., 2017 that "Few studies have documented the potential of including measurements of thermal neutrons (measured using the bare detector) [explaining that] for this to become standard practice, fundamental theoretical studies, concerning in particular footprint and atmospheric water vapor effects, are needed" [Andreasen et al., 2017; Desilets et al., 2017; Rosoleum et al., 2013; Andreasen et al., 2016]. However, they have contemplated that the bare (thermal) detector could be considered an approximation of water at or on the surface, like rain, snow, and vegetation [Zreda et al., 2012], and that continued work should attempt to derive the use of the bare detector from neutron data alone, without the need for samples [Zreda et al., 2012; Desilets et al., 2017].

However, there are some implementation differences. PNS instruments used on Earth are significantly larger than those used on Mars and the Moon, a design change intended to compensate for the low GCR flux at Earth's surface due to the atmosphere [T. Franz, personal communication, June, 2023]. It is also important to note that most terrestrial hydrology PNS instruments are not on mobile platforms, unlike planetary PNS instruments [Czarnecki et al., 2020, 2023; Hardgrove et al., 2011; Litvak et al., 2014; Mitrofanov et al. 2012; Tate et al., 2018, 2019; Ennico-Smith et al., 2020; Donaldson Hanna et al., 2023; Peplowski et al., 2023; Tuttle Keane et al., 2021; Martin et al., 2024a, 2024b; Elphic et al., 2008, 2015]. Though there are a few studies of mobile platforms, including one that utilized a typical terrestrial instrument mounted to a train [Schron et al., 2021], and another, smaller backpack-mounted version [Franz et al., 2015, 2018].

Planetary PNS has been conducted on Mars, onboard the Curiosity rover via the Dynamic Albedo of Neutrons (DAN) instrument [Litvak et al., 2014; Mitrofanov et al., 2012; Tate et al., 2018, 2019; Hardgrove et al., 2011; Czarnecki et al., 2020, 2023; Dibb et al., 2022, 2024; Berner et al., 2022, 2023, 2024], in addition to mapping subsurface H concentrations, results include catalogs of subsurface compositions when paired with the results from other instruments onboard the rover while searching the Gale Crater region of Mars [Tate et al., 2018, 2019; Czarnecki et al., 2020, 2023].

Unfortunately, planetary field analog experiments on Earth, whether utilizing passive or active methods, are few and far between. A few field tests of a rover-style active neutron spectroscopy prototype were conducted by NASA Ames [Elphic et al., 2008, 2015]. Since then, we have conducted several experiments in an effort to reunite the analysis of PNS methods in planetary and terrestrial hydrology [Gonzales and Hardgrove 2023, 2024a, 2024b], with the help of Dr. Vivioni's terrestrial hydrology team at ASU [Hurtado et al., 2023, 2024].

However, terrestrial hydrology instruments are otherwise very similar to that of planetary science, with a few exceptions (see Similarities and Differences of Terrestrial and Planetary Analog CRNS section), so using terrestrial correction factors for planetary analog field work with PNS detectors is feasible.

Goals and Objectives

Our goal is to utilize terrestrial hydrology corrections and methods for determining soil moisture and lattice water via PNS measurements at Earth's surface for planetary analog field experiments.

In order to do so, we must determine the spatial sensitivities of both RV detectors. This process requires examining whether the bare and moderated detectors have the same or different spatial sensitivities (radial, and surface proximity), and examining what effect orientation has on the spatial sensitivity.

Earth also has two factors unique to this work (of those studied with PNS thus far): an atmosphere with high concentrations of neutron moderators, and life itself (also referred to as biomass, it is mostly vegetation, though it can also be microbial, or even remnants of animals). Earth also has a magnetic field which also has an influence on GCR flux at the surface [Bazilevskaya et al., 1973; Desilets et al., 2006], unlike other worlds studied by PNS thus far, however that will not be considered herein.

Terrestrial hydrologists have already determined a series of correction factors to eliminate the effect of a neutron emitting and moderating atmosphere, which we apply before calculating SM.

We also need to characterize effects of vegetation in arid desert-like conditions, and determine whether future analog work will require correction factors for vegetation present.

Background

The Source of Neutrons for PNS.

PNS relies on Galactic Cosmic Rays (GCRs), generated by stars and supernovae and composed primarily of protons and alpha particles. When those high-energy GCRs reach the surface of a planet, they knock neutrons out of the material they encounter at high energies (around ~10^9 eV), a process defined as *spallation* [Prettyman, 2007]. The

exact definition of spallation is a little ambiguous amongst planetary scientists, but the process (later named spallation) can be traced back to the original study by Serber in 1947 [Serber, 1947; Shen, 1976].

Neutron Lethargy Spectrum.

As newly emitted, high-energy neutrons move around in the subsurface, they interact with the material they travel through via elastic scattering, and absorption. Elastic scattering reduces kinetic energy, typically via interactions with lighter elements (i.e. H, C, S, and N, among others). This neutron deceleration is called *moderation*, and the elements that elastically scatter neutrons are called *moderators*. As the neutrons continue to slow, they eventually reach speeds at equilibrium with the temperature of the material they travel through, and are referred to as *thermal neutrons*. One of the most effective moderators is H, as the mass and radius of a H atom is the closest to that of a neutron. Since H is also one of the most common elements in the universe, we can use moderated neutrons as a proxy for the H content of the subsurface. However, other common neutron scattering atoms include many light elements, like C and other elements common in biomass (plant, animal, and microbial life), which means that counts of neutrons are an indirect measurement of H abundance, and thus also an indirect measure of water. H is also common in several compounds, though water is one of the most prevalent, but others include hydroxyls (evidence of where water has been in the past), or acids (evidence of environmental changes in an area, though acids on Earth are often short-lived, reacting with bases and becoming water and sometimes then hydroxyls; but acids are more prevalent in the context of Venus with sulfuric acids clouds).

Absorption is when a neutron becomes a part of the nucleus of an atom, changing the isotope. Typically, absorption is most likely to happen when the neutron is traveling at slow speeds and interacts with heavier elements with several common isotopes. Some of the most common neutron absorbers are Fe and Cl, often found in iron oxides and salts.

These processes are shown in Figure 1.

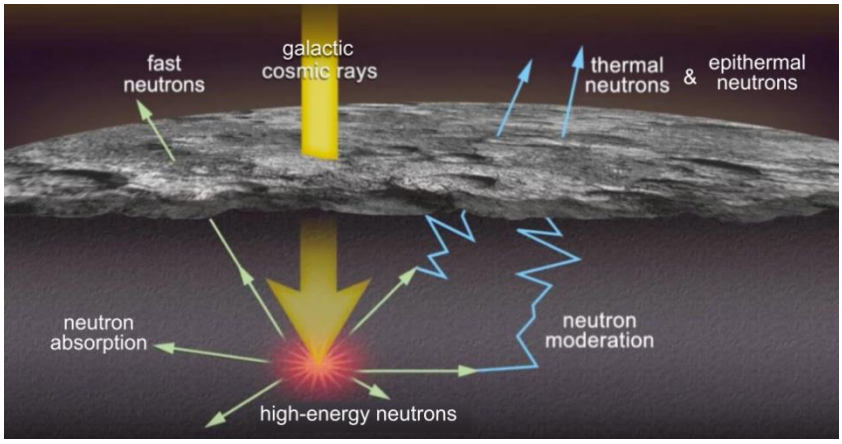

Figure 1. Spallation Emitted Neutrons (modified from [Parsons, 2020]). The generic process of neutron emission via GCRs. GCRs (primarily protons and alpha particles) are generated from stars and supernovae. When GCRs interact with a planetary surface, they knock neutrons out of the material, a process known as spallation. Those neutrons are traveling at high speeds, and are referred to as high-energy neutrons (see Neutron Lethargy Spectrum section). As they interact with the atoms that make up the material they are traveling through, neutrons get either absorbed or elastically scattered. Elastically scattering, slows them down, called "neutron moderation". Neutrons that remain within 1 m of the surface have a chance of scattering back out of the surface and can be detected. As the neutrons emerge from the surface, they can be in one of three energy bins "fast", "epithermal", or "thermal" neutrons.

When neutrons are produced by spallation, they have a high-energy ($> 10^7$ eV). According to the kinetic energy equation $KE = ½ mv^2$, since the mass of the neutron is a constant, the kinetic energy can be directly translated into speed. Elastic scattering is

commonly attributed to lighter elements, while absorption is commonly associated with heavier elements with many isotopes. The lower the energy (and thus the lower the speed), the more likely they are to be absorbed instead of elastically scattered. Moderation creates a spectrum of energy ranges that provide information about the elemental abundances of the subsurface, called the Neutron Lethargy Energy Spectrum.

Figure 2 (a), below, shows the energy ranges of neutrons emanating from the surface of the Moon (analogous to Mars as well), while (b – e) show a variety of scenarios on Earth, and (f) exemplifies the “water sensitive domain”.

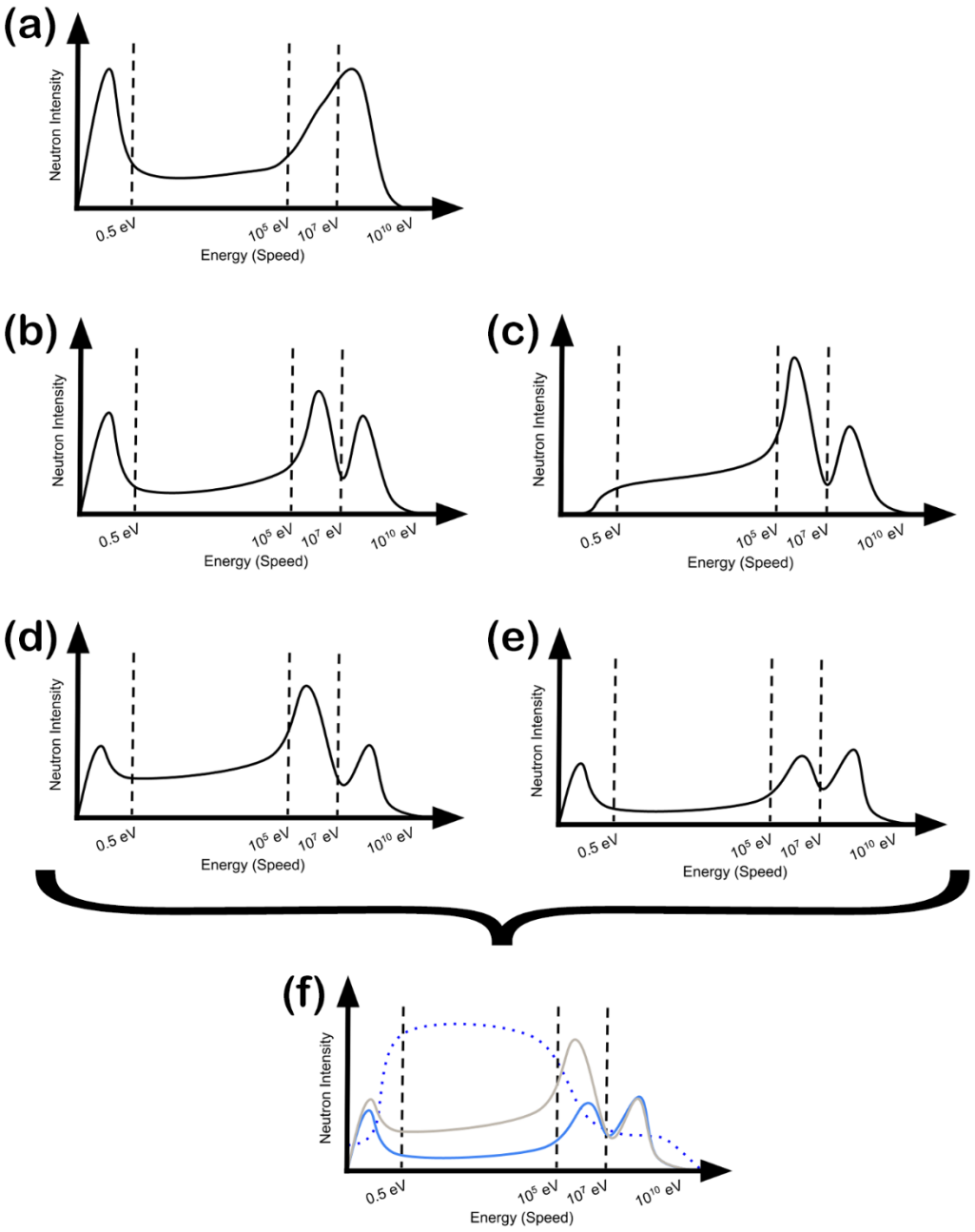

Figure 2. Neutron Lethargy Energy Spectra in a Variety of Scenarios. As simulated from orbit around the Moon (a) [adapted from Feldman et al., 1998], as measured on Earth at the surface (b) and 12 km above the surface via aircraft (c) [b and c adapted from Goldhagen et al., 2002], as simulated on Earth with 1 weight percent (wt %) WEH (d) and 50 wt % WEH (e), and the ratio between (d) and (e) shown in (f) to demonstrate the water sensitive domain [d, e, and f adapted from Weimar et al., 2020].

In Figure 2 (a) the peak on the right-hand side of the spectrum (the highest energy peak) is the speed at which neutrons are initially traveling after GCRs knock them from their host isotopes [Goldhagen et al., 2002]. Neutrons $>10^7$eV are called high-energy. As neutrons continue to decelerate via moderation, they form a flatter slope, this zone of gradual deceleration is considered the epithermal region (0.5 eV - 10^7eV). Eventually, neutrons slow to speeds that match the temperature of the material they travel through, achieving thermal equilibrium (< 0.5 eV). The left-most peak is from the thermal neutrons.

Figure 2 (a) shows the neutron energies seen on a world with a thin (or negligible) atmosphere, though the precise atmospheric thickness boundary for neutron emission and moderation eludes a preclusive definition at present. At some yet unknown point (likely related to the atmospheric temperature and pressure at which water and other volatiles become stable at the surface of a rocky world), a volatile-rich atmosphere becomes thick enough that the emission and moderation of neutrons in the atmosphere creates a new peak on the neutron lethargy spectrum, as exemplified by Figure 2 (b – e).

In Figure 2 (b), the thermal neutron peak (farthest left) remains, and there is also a new peak to the left of the high-energy peak. In the curves measured above the surface, the thermal neutron peak is no longer present. The neutrons at that energy no longer have enough energy to reach the detector when it is 12+ km above the Earth's surface (Figure 2, c) before getting absorbed. However, in the spectrum measured via aircraft (Figure 2, c), the peak of neutrons from the atmosphere is taller, indicating that there is a higher concentration of neutrons at these energies in the atmosphere, and confirming that the origin of this peak is the presence of the thick atmosphere. This peak is considered the

fast neutron energy range (10^5 eV – 10^7 eV). Refer back to the epithermal domain, which includes this region. Fast neutron energies are considered a subset of the epithermal range.

Now that the sources of the three peaks have been verified, return to the interconnecting slope of the epithermal zone, branching between the thermal neutrons and the higher energy neutrons. This segment is present in 3 scenarios

1. When a world has a negligible atmosphere (Figure 2, a),
2. When at the surface of a world with a non-negligible atmosphere where GCRs can still reach the surface (Figure 2, b),
3. When still in that atmosphere, many km above the surface (Figure 2, c).

This flatter segment is from neutrons emitted and moderated in the subsurface that bounce back out before achieving thermal equilibrium with the surface material itself. Figure 2 (d, e, and f) demonstrate the variation due to variations in water content in this segment.

Figure 2 demonstrates that it is the height of each of the four energy ranges, relative to the other ranges, that indicates concentrations of moderators and absorbers in the subsurface and atmosphere. In the Materials, Methods, and Discussion section, the following ranges (also shown in Figure 2) will be used as an approximate definition of neutron lethargy spectrum energy ranges. Thermal neutrons will be considered < 0.5 eV, approximated from Andreasen et al. 2016, 2017, Tate et al. 2019, and Hardgrove et al. 2011. Epithermal neutrons will be defined as 0.5 eV to 10^7 eV, adapted from Andreasen et al., 2017 and Goldhagen et al., 2002. Fast neutrons, a subset of epithermal, will be defined as 10^5 eV to 10^9 eV, as suggested by Goldhagen et al. 2002, Andreasen et al.

2017, and Weimer et al., 2020. High-energy ranges will be considered those above 10^7 eV, though it is usually depicted as tapering off at or before the 10^{10} eV mark.

The water sensitive domain (Figure 2, f) is the region of interest to terrestrial hydrologists. They set up stationary detectors for long periods of time, often years, to measure the precipitation and soil moisture (defined as water between the grains of the soil, but not including any water in the crystal lattice of the minerals; abbv. SM) affecting a region over a long period of time. They use a plethora of samples to remove the counts from H that are locked in the crystal lattice (called Lattice Water; LW), and C left behind as remnants of organics (Soil Organic Carbon; SOC) not including vegetation (which is corrected for separately if needed).

A study in South Africa in 2020 setup PNS instruments in an area that had been allowed to grow a forest during an 11-year clearing hiatus. Trees were clear-felled via burning, and felled trees were removed from the field of view of the detectors (see Radial Sensitivity section for more information on field of view). All trees in the vicinity of the instruments were removed from the area in a short period of time. The results were recorded by two PNS instruments, one 2 m above the surface, one 18 m above the surface, both mounted to the same tower, see Figure 3, below [Vather et al., 2020].

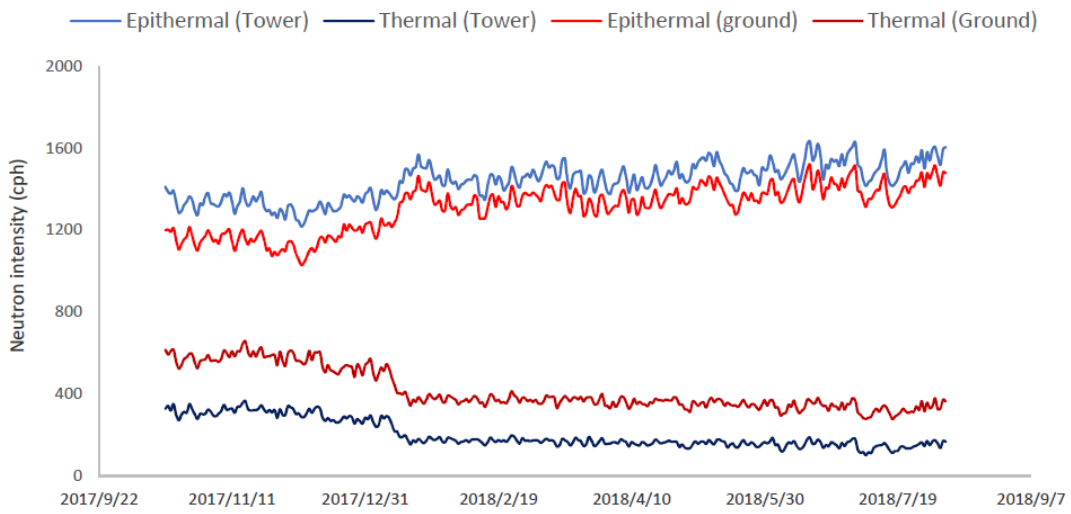

Figure 3. Epithermal and Thermal Neutron Intensity Fluctuations as Measured Before and After Vegetation Removal from [Vather et al., 2020]. Both PNS instruments saw an increase in epithermal neutrons and a decrease in thermal neutrons after the trees were removed. Also note that the instrument placed farther from the surface (tower-mounted, blues) detects fewer thermal neutrons and more epithermal neutrons compared to the instrument nearer to the ground. Small variances in the neutron counts are due to natural fluctuations in GCRs seen regardless of the world on which measurements are conducted.

Vather et al., 2020 results (Figure 3), suggest that both detectors are sensitive to vegetation, and react oppositely. Also note that the detector farther from the surface sees fewer thermal neutrons and more epithermal neutrons in general, reflecting the same patterns seen in Goldhagen et al., 2002 as their detectors were moved to elevations farther from the surface.

Planetary hydrologists use a comparison between the thermal and epithermal energy regions as a measure of elemental abundances of neutron moderators and absorbers within the subsurface [Tate et al., 2018]. Mobile planetary detectors include orbiters like Lunar Prospector's Gamma Ray Neutron Spectrometer (GRNS) [Feldman et al., 1998 and 1999], and the Mars Odyssey High Energy Neutron Detector (HEND) [Feldman et al., 2002; Mitrofanov et al., 2002], among others, or rovers like Curiosity

(Dynamic Albedo of Neutrons or DAN instrument) [Litvak et al., 2014; Mitrofanov et al., 2012; Tate et al., 2018, 2019; Hardgrove et al., 2011; Czarnecki et al., 2020, 2023; Berner et al., 2022, 2023, 2024; Dibb et al., 2022, 2024] currently on Mars, and the upcoming South Pole Hopper [Martin et al., 2024a, 2024b], Endurance [Tuttle Keane et al., 2021], Lunar-VISE [Donaldson Hanna et al., 2023; Peplowski et al., 2023], and VIPER [Ennico-Smith et al., 2020], several of which are expected to land on the Moon within the next few years. Mobile, planetary instruments measure changes in the thermal and epithermal neutron counts indicating a change in subsurface composition as the instrument platform traverses. This change in neutron count rates is considered the Water Equivalent Hydrogen (WEH), defined as subsurface changes that could be related to concentrations of hydrogen, particularly in water, which can include both H filling the pore spaces between grains (terrestrial SM) and H in the crystal lattice structure of the grains themselves (terrestrial LW).

Atmospheric Corrections.

In cases like the Moon and Mars, their atmospheres are not thick enough to create a peak of fast energy neutrons that can be differentiated from the high-energy peak and the gradual slope of the water sensitive domain, and thus the atmosphere is considered negligible to the neutron count rate. However, for cases like Earth, where the atmosphere is thick enough to create a peak in the fast energy subset of epithermal energy ranges, there are a series of correctional equations and simulation-based constants to remove counts from neutrons emitted and moderated above the surface from the moderated detector count rates [Rosoleum et al., 2013]. Terrestrial hydrology has a standardized

method for this [Andreasen et al., 2016, 2017; Franz et al., 2012, 2013, 2015, 2016, 2018; Hurtado et al., 2023, 2024; Schreiner-McGraw et al., 2016; Vather et al., 2018, 2020; Zreda et al., 2008, 2012], though these correction factors are specific to Earth's atmospheric conditions. Corrected count rates can then be used to calculate WEH and SM on Earth.

First, determine the reference pressure (P_{REF}) of the atmosphere in units of Pa, using the latitude, longitude, and elevation of the field site (COSMOS measurements utilize a pre-built calculator found here: https://crnslab.org/util/intensity.php, [Franz et al., 2012] though this site produces estimates in mb). Then use the reference pressure and high-energy neutron attenuation length (λ), which is assumed to be 130 g/cm^2 in the northern hemisphere of Earth [Desilets et al., 2006], and measured air pressure (P_{AIR}) in units of Pa (or g/cm^2), to correct for air pressure using (1).

$$P_{CF-AIR} = exp\left(\frac{P_{AIR}-P_{REF}}{\lambda}\right) \quad (1)$$

Then use the actual air temperature (T_{AIR}) in Celsius, and the following best fit formula originally from Bolton, 1980, to calculate the maximum potential saturation pressure of water vapor at the field site (in Pa).

$$P_{SAT} = 6.112 * exp\left(\frac{17.67*T_{AIR}}{243.5+T_{AIR}}\right) \quad (2)$$

Maximum potential saturation pressure can then be multiplied by relative humidity (RH, measured as a percent) to determine the actual pressure from water vapor at the field site, again in Pa [Rosoleum, et al., 2013].

$$P_{ACT} = \left(\frac{RH}{100}\right) * P_{SAT} \quad (3)$$

Then, using the universal gas constant for water vapor (R_{VAP}) in J/K/kg, the actual measured air temperature (T_{AIR}, measured in Celsius, then converted to kelvin), and the actual water vapor pressure (P_{ACT}) from (3), absolute humidity of the air (ρ_{VAP}) in units of kg/m^3 can be calculated via the ideal gas law in units of g/m^3 (4) [Rosoleum et al., 2013].

$$\rho_{VAP} = \left[\frac{P_{ACT}}{R_{VAP}(T_{AIR}+273.15)}\right] * 1000 \quad (4)$$

Then the correction factor for variations in the atmospheric water vapor can be determined (in g/m^3), utilizing the results from (4), and the following equation from Franz et al. 2012 and Franz et al., 2013 derived from Monte Carlo N-Particle transport model (MNCP) simulation best-fit equation.

$$WV_{CF} = 1 + 0.0054 * \rho_{VAP} \quad (5)$$

High-energy neutron intensity rates are measured hourly by a NM64 neutron monitor located in Jungfraujoch, Switzerland (https://nearfld.com/reguser/unl_2/ Roric2 IMEI 4260, kindly provided by Physikalisches Institut, University of Bern, Switzerland, additional information can be found here: https://www.nmdb.eu/station/jung1/) and are used as a global constant to correct for fluctuations in neutron counts at the surface of Earth (F_{SOL}, solar flux), as suggested by Franz et al., 2012. The F_{SOL} values for the UTC time corresponding to data collection are averaged, then factored into (6) along with the water vapor correction factor (WV_{CF} from 5), air pressure correction factor ($P_{CF\text{-}AIR}$, from 1), a constant scaling factor (CSF) for neutron intensity from the same COSMOS calculator as the reference pressure (see 1), and the raw neutron count rate (N; counts per min or hour, cpm or cph) to produce a corrected neutron count rate (cpm, or cph, to match units of N).

$$N_C = \frac{N * WV_{CF} * P_{CF-AIR} * F_{SOL}}{CSF} \quad (6)$$

This corrected neutron count rate has accounted for and removed neutrons emitted and moderated in the atmosphere. In other words, we have effectively removed the peak from neutrons emitted and moderated above the surface in the neutron lethargy spectrum (see Figure 3). The remaining counts from neutrons emitted and moderated in the subsurface and will be used to determine the SM and WEH.

Calculating SM and WEH.

Recall that neither the bare nor moderated detector measure purely one neutron energy range. Naming them thermal and epithermal detectors, respectively, is simply a reference to the energy range from which the majority of neutrons are counted. There are equations to describe the contributions of thermal and epithermal counts to the neutron counts measured by both detectors that can be found in [Vather et al., 2020; Andreasen et al., 2020], but they will not be used here, as the time spans are too short and the counts per minute are low enough that the signal from the non-dominant energy range is considered negligible (see Figure 5 explanation for additional information about low count rates).

From this corrected neutron count rate, the WEH and SM of the subsurface can be calculated. Constants in the following soil moisture calibration equation (7) are derived from MCNPX simulations from Desilets et al., 2010 to best approximate fast to epithermal neutrons moderated by water in silicic or sandy conditions.

To account for and remove any water in the grains of the soil, samples are used to determine SOC and LW with units of g(LW or SOC)/g(soil) which are subtracted from

the volume-ratio that is the neutron count rate, in the calibration equation, before multiplying by the bulk soil density (ρ_{bd}, g/cm^3, pore space between the grains, also from the samples), thus adapting the equation to determine the actual SM content in silicic and non-silicic environments [Franz et al., 2013], which is considered a volumetric weight percent (wt %).

$$SM = \left[\frac{0.0808}{\left(\frac{N_C}{N_0}\right)-0.372} - 0.115 - (LW - SOC)\right]\rho_{bd} \quad (7)$$

To correct for any additional, unexpected neutron flux changes at the field site, the corrected neutron count rate is divided by the ideal neutron count rate in dry, silicic conditions (N_0), which is calculated using the same equation (7), and assuming LW and SOC to be 0, and replacing N_0 with the average of actual neutron counts during the experiment.

Recall that COSMOS detectors are typically stationary instruments, which allows the user to assume that the geochemistry remains a constant, and can thus be subtracted from the equation. For a mobile detector, it is wiser to assume that the geochemistry is allowed to change and may influence the neutron count rate and therefore the final calculation. In other words, mobile detectors need determine the WEH rather than the SM.

WEH can be achieved using a modified version of the SM equation (8), similar to that found in [Bogena et al., 2013]. WEH expresses fluctuations in neutron count rates as the result of:

1. H present in the crystal lattice structure (LW),
2. H in a liquid form, filling the pore space between the grains (SM), or

3. if there are other common moderators present in the soil geochemistry (primarily accounted for via the SOC correction factor).

$$WEH_T = \left[\frac{0.0808}{\left(\frac{N_C}{N_0}\right)-0.372} - 0.115\right]\rho_{bd} \quad (8)$$

WEH is used to describe the quantities of moderators in the subsurface. In planetary science, it is also used in conjunction with the sample data in order to determine the composition of the surface in one or two layer models within 0.5m of the surface of a world [Czarnecki et al., 2020, 2023; Tate et al., 2018, 2019], and within the detector field of view (FOV). More on FOV in the Radial Sensitivity section.

In planetary science, an experimental relationship has been derived between WEH and epithermal neutron count rates. This is shown in (9), where k is a unitless compositional constant that is a function of the density, composition and regolith properties of the planetary body and is defined in units of μg/g [Prettyman et al., 2012; Feldman et al., 1998], thus WEH is provided in units of μg/g, another volumetric weight ratio.

$$WEH_P = k\left[\left(\frac{N_0}{N}\right) - 1\right] \quad (9)$$

To correct for the Earth's atmosphere and determine WEH during field analog traverses on Earth in this work, (8) will be used in later sections.

Whether the terrestrial or planetary equation is used, both are greatly dependent on the FOV of the detector itself.

Radial Sensitivity.

On both Earth and Mars, the FOV (sometimes called the “footprint”) is defined based on simulations. It extends up to 1 m below the surface, maximum, and in a radius of sensitivity above the surface.

Depending on the altitude of the neutron detectors, one can increase or decrease the pixel scale of the data. From orbit, detectors can measure tens to hundreds of kilometers per pixel. Comparatively, if the detectors are moved to within ~2 m of the surface, that can be reduced to the scale of hundreds of meters [Andreasen et al., 2017; Desilets and Zreda, 2013; Kohli et al., 2015; Zreda et al., 2008] to individual meters [Czarnecki et al., 2020, 2023; Hardgrove et al., 2011; Litvak et al., 2014; Mitrofanov et al. 2012; Tate et al., 2018, 2019], depending on the rocky world in question, presence of a neutron emitting and moderating atmosphere, and the type and size of the detectors used (Figure 4).

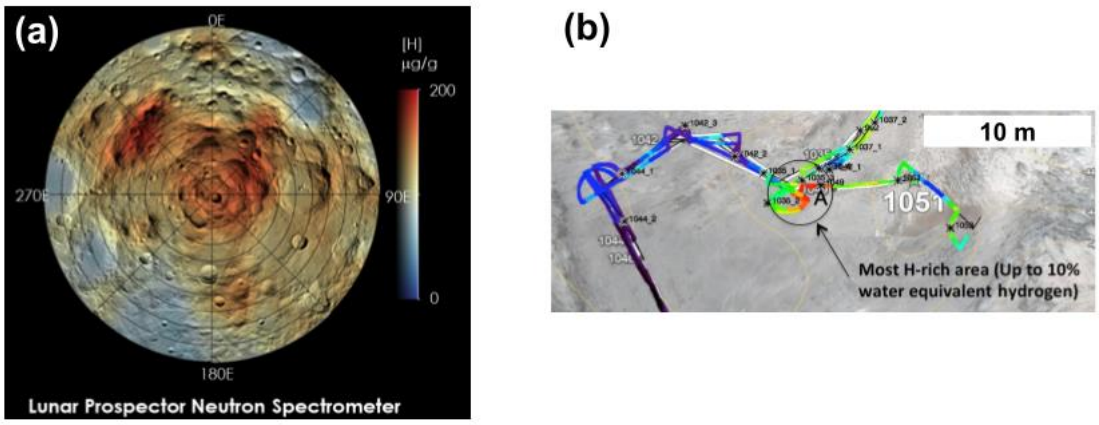

Figure 4. WEH Maps from Detectors in Orbit and On the Surface. Both maps show high concentrations of WEH in red, low concentrations in blue. Scales of the Lunar Prospector map of the South Pole of the Moon (a) are tens of km per pixel [Feldman et al., 2001]. Comparatively, the scale of the DAN data in (b) is at scales of 1-3 meters, indicating the path the Curiosity rover took through this particular station [Czarnecki et al., 2020].

For the DAN instrument onboard the Curiosity rover, this footprint extends 1-3 m's from the rover and ~0.5m into the subsurface [Tate et al., 2018, 2019; Czarnecki et al., 2020, 2023; Hardgrove et al., 2011; Mitrofanov et al., 2012; Litvak et al., 2014, 2020; Berner et al., 2022, 2023, 2024; Dibb et al., 2022, 2024]. Earth-based PNS have radii on the field-scale, ~130 - 240 m [Andreasen et al., 2017; Kohli et al., 2015; Desilets and Zreda, 2013], two orders of magnitude larger than the DAN instrument (~1 – 3 m) Tate et al., 2018, 2019; Czarnecki et al., 2020, 2023; Hardgrove et al., 2011; Mitrofanov et al., 2012; Litvak et al., 2014, 2020; Dibb et al., 2024].

On Earth, the simulations and field tests of radial sensitivity [Andreasen et al., 2017; Desilets and Zreda, 2013; Kohli et al., 2015; Zreda et al., 2008; T. Franz, personal communication, June 5th, 2023], have produced a method for quickly approximating the radial sensitivity of a Cosmic Ray Neutron Spectrometer (CRNS) instrument. By setting up the instrument over a large "pool" (concentrated source of H in the environment) of moderators [Bogena et al., 2013], i.e. a lake, and stepping the instrument gradually towards the edge and then away from the pool, the neutron count rate produces an exponential curve where neutron counts are lower with higher concentrations of WEH. This can be simulated via equations (8) and (9) as demonstrated in Figure 5, below.

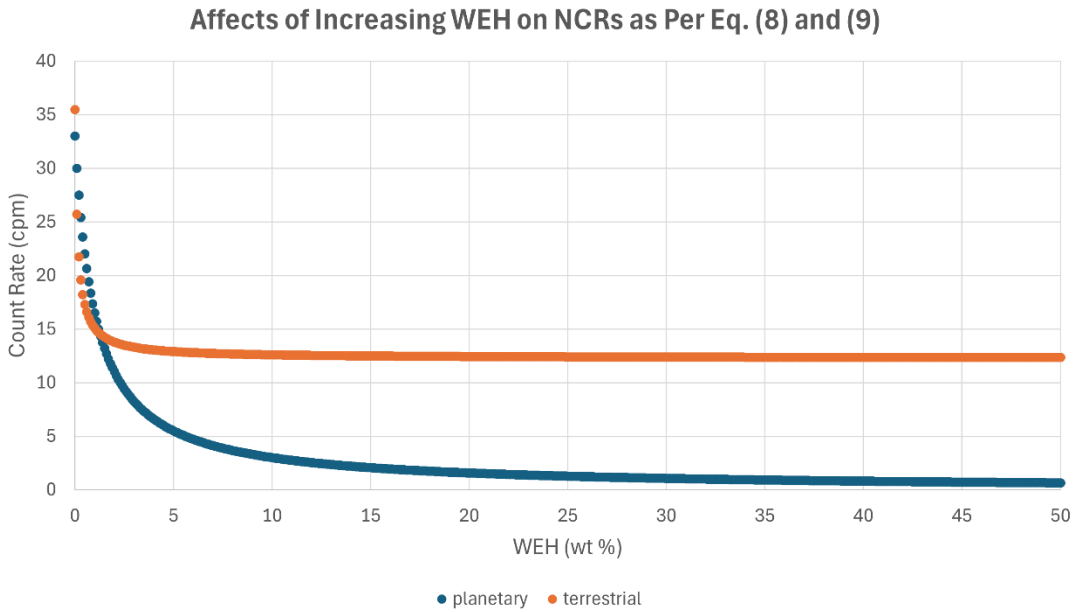

Figure 5. WEH Comparison Between Planetary PNS and Terrestrial Hydrology PNS. WEH curves using the equations from terrestrial hydrology (8; with k = 1; orange) and planetary science (9; blue). Increasing WEH in both equations produces a similar exponential curve. The asymptotic behavior of the terrestrial curve is the result of the constants in the terrestrial equation (8) that approximate the shape of the neutron scattering curve on Earth, due to the presence of an atmosphere that is both capable of emitting neutrons via interactions with GCRs and is composed primarily of neutron moderators. Though, neither planetary science nor terrestrial hydrology can successfully calculate WEH from a count rate that is too low. Thus, we can use ~15 cpm (before atmospheric corrections are applied) from the asymptotic behavior of the terrestrial WEH curve as a minimum cutoff for both scenarios, suggesting any data below that rate is too low to calculate an accurate WEH of the subsurface.

From a statistics standpoint, the majority of the neutrons from the source of moderators producing an exponential decay curve emanate from within two exponential folds, or two e-fold lengths approximated by the following equation [Zreda et al., 2008; Desilets and Zreda, 2013].

$$\left(1 - \frac{1}{e^n}\right) * 100 \qquad (10)$$

When n = 2 (for 2 exponential folds), the equation solves to 86%. To determine the radius from the plotted, raw data, fit an exponential shape to the curve produced with

count rate on the y-axis and distance from moderator pool on the x-axis. Then subtract the minimum neutron count rate (over or near the water) from the maximum neutron count rate (over dry land), and multiply by 0.86. Then use the calculated count rate, trace it to the exponential curve fitted to the data, and determine the distance from the water to find the approximate radius of sensitivity (see Radial Sensitivity Test sections for a numerical implementation).

CHAPTER 2

MATERIALS, METHODS, AND RESULTS

Materials

Introduction to the Instruments.

A typical neutron spectrometer instrument consists of a pair of detectors, one of which primarily measures thermal neutrons, and the other primarily measures epithermal neutrons or a combination of epithermal and thermal neutrons from which a quantity of epithermal neutrons can be calculated. The individual detectors are typically denoted by the energy range of neutrons they are most sensitive to in order to differentiate them. While there are many different types of neutron spectrometer detectors, this work utilizes ^{3}He proportional counters.

Proportional ^{3}He Detectors.

The neutron detectors used herein are ^{3}He-filled, gas detectors common amongst both terrestrial hydrology and planetary science communities [Andreasen et al., 2016]. ^{3}He is particularly good at detecting thermal neutrons [Knoll, 2000].

Any neutrons that have already been moderated by H and other neutron moderators in the subsurface are travelling at sufficiently low speeds to be absorbed by the ^{3}He, generating a small zap of energy, which the detector 'counts'. The raw data produced is a measurement of the number of neutron counts detected in a set period of time (i.e. counts per hour or counts per minute).

One detector is wrapped in boron, which absorbs most neutrons with energies <1 eV [Andreasen et al., 2016]. The B further limits the range of neutrons that will pass through the sensors, removing anything traveling at a rate too slow to be considered a

measurement of the element(s) in question (usually H). It acts similarly to the Cd on the DAN detector onboard the Curiosity rover, which also filters out the low-speed thermal neutrons [Czarnecki et al., 2020, 2023; Hardgrove et al., 2011; Litvak et al., 2014; Mitrofanov et al. 2012; Tate et al., 2018, 2019; Dibb et al., 2024].

This B-wrapped detector is also wrapped in high density polyethylene [HDPE; a common hydrocarbon, with the formula $(C_2H_4)_n$], a neutron moderator. The job of the HDPE neutron moderator is to reduce the speed of neutrons traveling too fast to interact with the ^{3}He [Andreasen et al., 2016], primarily epithermal (and fast) from which it derives its name: the epithermal or moderated detector.

The other detector has neither the B nor the HDPE, and is often referred to as the unmoderated or bare detector. The counts from this detector are considered an approximation of the thermal neutron population.

Figure 6 exemplifies the respective filtering and moderating properties of detector components, while Figure 7 shows the neutron energies measured on the lethargy spectrum.

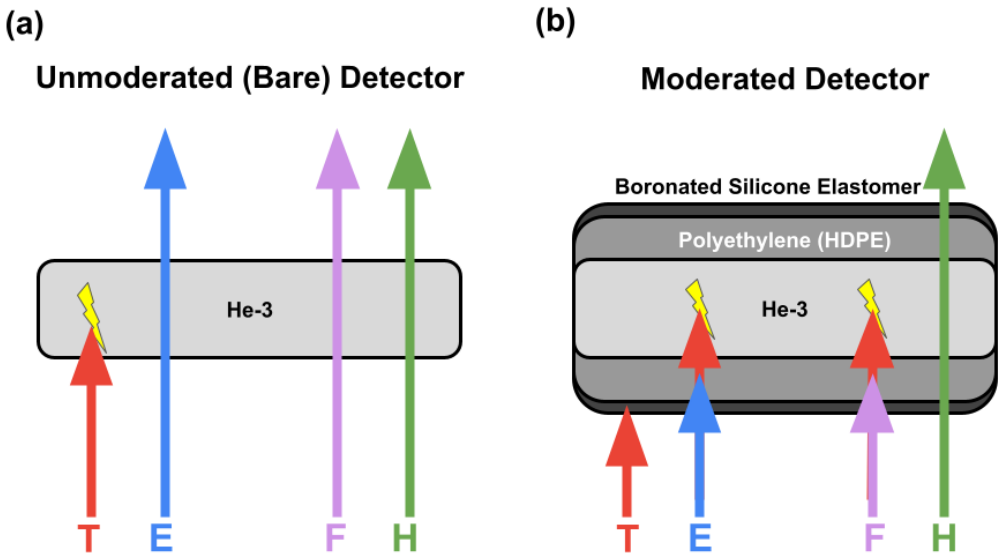

Figure 6. ^{3}He Proportional Counters and Neutron Energies. From left to right, thermal (T, red), epithermal (E, blue), fast (F, purple), and high-energy (H, green) neutron energy range interactions with both detectors. In the unmoderated or bare detectors (a), only the thermal neutrons are traveling at speeds that will be absorbed by the ^{3}He. All other neutron energies are traveling too quickly, and pass through the detector without getting absorbed by the ^{3}He. In the moderated detectors (b), the thermal neutrons are filtered out (absorbed) by the boronated silicone elastomer, which all other energies pass through. Just inside the boron, sit four sheets of HDPE, which slow down the epithermal and fast neutrons to speeds that the ^{3}He can absorb (thermal speeds, red), while the high-energy neutrons continue to pass through the detector, undetected.

The PNS instruments in this experiment use a pair of ^{3}He filled gas tubes of the above specifications.

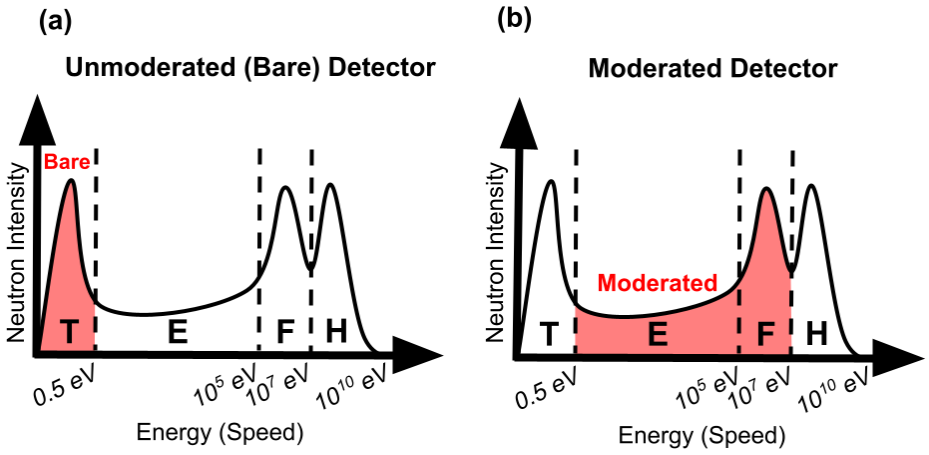

Figure 7. Neutron Energy Ranges and Detector Sensitivity Ranges. As was described above, the two detectors are sensitive to different domains on the neutron lethargy spectrum. The dashed line between thermal and epithermal neutron zones in this figure is an approximation of the boron cutoff, in this experiment, which can be considered analogous to the Cd cutoff used by the DAN instrument [Czarnecki et al., 2020, 2023; Hardgrove et al., 2011; Litvak et al., 2014; Mitrofanov et al. 2012; Tate et al., 2018, 2019; Dibb et al., 2024].

The standardized terrestrial hydrology atmospheric correction factors (see Atmospheric Corrections section, above), are used to effectively alter the lethargy spectrum removing the influence of neutrons emitted and moderated above the surface (Figure 8, below), which means the resultant data more closely resembles the spectrum seen on other rocky worlds without a thick atmosphere (Figure 2, a).

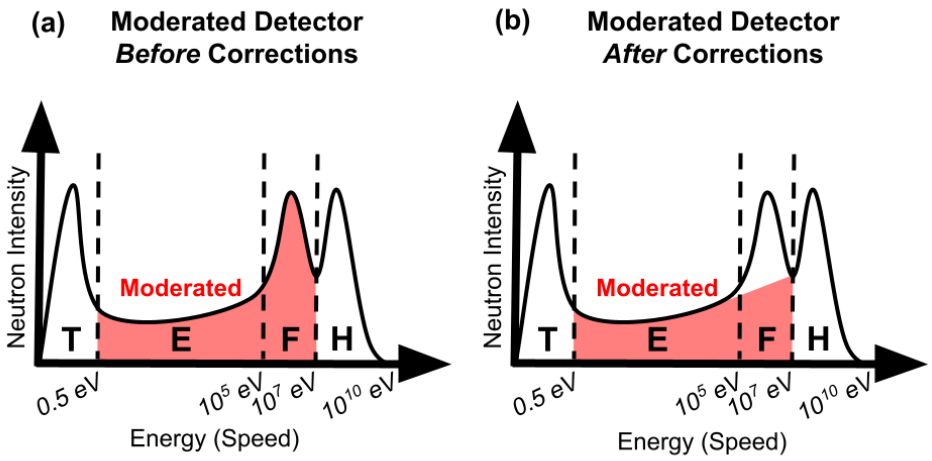

Figure 8. The Neutron Lethargy Spectrum Before and After Atmospheric Correction Factors are Applied to the Moderated (Epithermal) Data. The peak from neutrons emitted and moderated above the surface is effectively removed from the raw data collected by the moderated detector (highlighted in red in a) using the atmospheric corrections (1-6, in the Atmospheric Corrections section, above), resulting in an updated sensitivity range (red zone in b), and allowing the resultant corrected counts to be used to calculate the SM and WEH (equations 7-9).

The atmospheric corrections are standardized and applied to all PNS instruments used by terrestrial hydrologists, regardless of whether they are ^{3}He filled or not [Andreasen et al., 2016, 2017; Franz et al., 2012, 2013, 2015, 2016, 2018; Hurtado et al., 2023, 2024; Schreiner-McGraw et al., 2016; Vather et al., 2018, 2020; Zreda et al., 2008, 2012; Bogena et al., 2013; Desilets et al., 2006, 2010, 2013, 2017; Kohli et al., 2015; Rosoleum et al., 2013; Schron et al., 2017; Weimar et al., 2020; Goldhagen et al., 2002; Iwema et al., 2021].

Note, all energy ranges described with respect to detector sensitivity ranges are approximate. Detector cutoffs specified are not exact. The bare detector includes some contribution from the epithermal neutrons, and the epithermal detector includes some contribution from the thermal neutrons. Equations to extract ratios of contributions from

both energy ranges to both detectors exist [Vather et al., 2020; Andreasen et al., 2016], however they will not be used herein. Because the count rates measured by the portable detectors at the cpm rate are close to the cutoff range described by the asymptotic behavior of the curves in Figure 5, contributions from the non-dominant energy ranges are considered negligible.

As shown in Figure 9, below, there are two different PNS instruments (detector pairs, one moderated one unmoderated) used in this series of experiments.

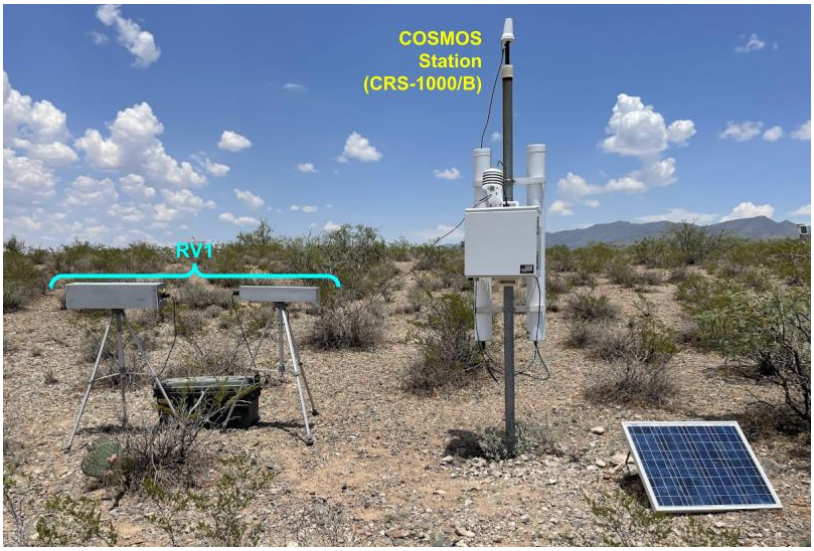

Figure 9. The Two PNS Instruments Used Herein: COSMOS and RVs. On the right is the COSMOS instrument, and on the left is the RV instrument, both of which will be described in the following sections. Both of these instruments are Proportional ^{3}He Instruments with one thermal and one epithermal detector as per the above description, see below for instrument specifics.

COSMOS CRNS.

The COsmic-ray Soil Moisture Observing System (COSMOS) [Zreda et al., 2012] was developed by Hydroinnova and Questa Instruments for use as a stationary, regional PNS, providing year-round data for various locations around the world, accessible via

Iridium satellite for remote data collection and cataloging [Zreda et al., 2012; Hydroinnova, 2013]. There are several COSMOS detectors in the southwestern United States setup by Dr. Enrique Vivoni's terrestrial hydrology team at Arizona State University, one of which can be found at the Long Term Ecological Research (LTER) site in the Jornada Basin of NM, and was utilized for this study. It was installed at a small playa in the summer of 2022 [Hurtado et al., 2023, 2024; Gonzales and Hardgrove 2023, 2024a, 2024b], similar to the COSMOS instrument seen in Figure 9, and in later figures.

Each individual COSMOS neutron detector is 122.5 cm in length [Hydroinnova, 2013], and has a radial sensitivity or footprint of ~130-240 m [Andreasen et al., 2017; Kohli et al., 2015]. Regional hydration can play a role in the spatial sensitivity, as more arid, desert conditions lead to fewer moderating neutron interactions and therefore a larger footprint, while humid, wet conditions lead to more moderating neutron interactions and a smaller footprint [Iwema et al., 2021]. The COSMOS instrument records neutron counts in hourly rates [Hydroinnova, 2013].

While these terrestrial detectors are usually stationary, they can be used in a mobile fashion. One such study attached a COSMOS instrument to a train [Schrön et al., 2021], and another used a backpack instrument [Franz et al., 2018], similar to the one described below.

RVs.

The new instruments, two field-portable PNSs that we are testing were also developed by Hydroinnova and Questa Instruments for custom use as a mobile instrument meant to imitate either an instrument suite during either a planetary rover or

manned exploration mission. They are designed to be small, portable versions of the COSMOS instruments, called rovers (RVs). Each detector is 56.2 cm in length, and battery powered. These detectors are encased in sealed, aluminum boxes, for durability. In Figure 9, the moderated tube is notably larger than the unmoderated tube due to the four, 0.25 inch layers of removable HDPE shown in, Figure 10, three of which are removable. For the tests performed herein, all four layers of HDPE were left in the moderated sensor, with the exception of the moderator thickness test. These instruments record neutron counts per minute [Gonzales and Hardgrove, 2023, 2024a, 2024b].

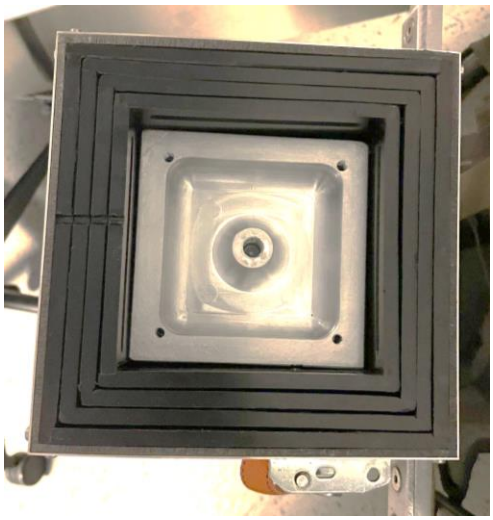

Figure 10. Polyethylene Moderator in the Moderated RV Detectors. The ^{3}He tube, inside the metal box at the center, is encased in four sheets of 0.25 inch HDPE, which is all wrapped in one 0.125 inch boron silicone elastomer with a 25% boron content to filter out neutrons in the thermal ranges, called a boronated thermal neutron shield, which ensures that the moderated detector is measuring neutrons in the water sensitive domain (epithermal) and not below it (thermal).

There are two separate instruments, each referred to as rovers (hereby deemed RV1 and RV2; see Figure 11, below). Both RV instruments are usually mounted

horizontally via tripod (see Figures 9 and 11), designed to imitate the arrangement used on the Curiosity rover [Litvak et al., 2014; Mitrofanov et al., 2012] with the goal of maximizing the amount of detected neutrons emanating from the surface directly below the detectors.

As is shown in Figure 11, RV2 can also be mounted vertically using the backpacks instead of the tripods, which also aids portability.

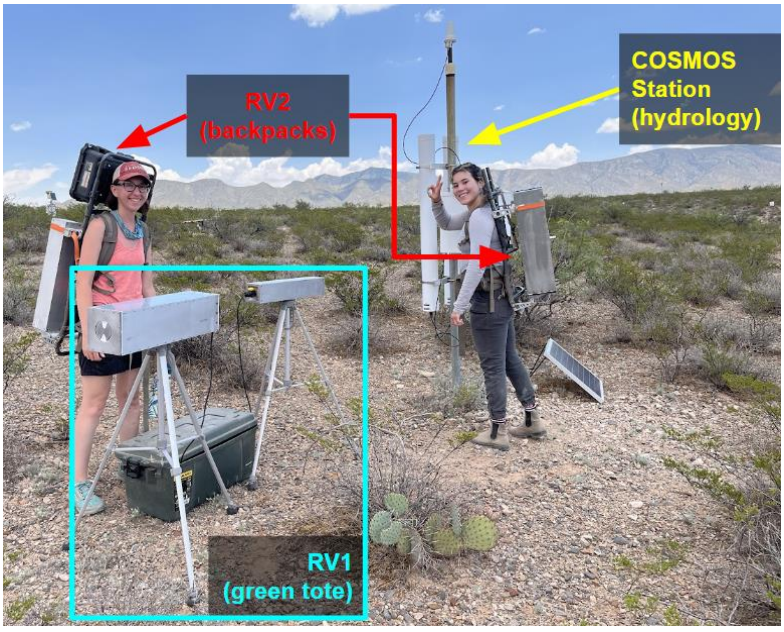

Figure 11. Both RV Instruments and the COSMOS Instrument. These same instruments are used in [Gonzales and Hardgrove, 2023, 2024a, 2024b]. On the left is the first author. On the right is a member of Dr. Enrique Vivoni's hydrology team at ASU, and author of [Hurtado et al., 2023, 2024] on the COSMOS data collected at some of the same field sites used in this study. Note that the COSMOS detectors are approximately twice the length of the RV detectors. Both are ^{3}He proportional counters.

The RV units have four configurations, three of which are shows in Figure 12

1. tripod-mounted horizontal
2. tripod-aided vertical

3. cart-mounted horizontal
4. set directly on the ground, also horizontal (not shown in Figure 12)

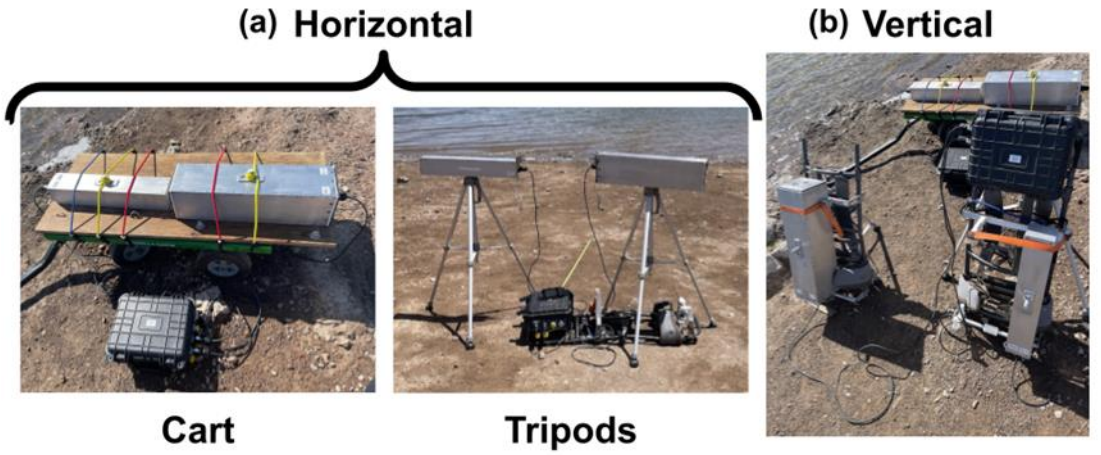

Figure 12. The Various Configurations of the RV Instruments. There are two horizontal configurations (a) and one vertical orientation (b) used during data collection herein. From left to right, cart-mounted horizontal, tripod-mounted horizontal, and tripod-assisted vertical.

Note that the backpack-mounted carrying configuration shown in Figure 11 is not used during data collection as humans constitute a large collection of moderators that would be too close to the instruments if used in that configuration during data collection.

As is evident from the configurations shown in Figure 11 and Figure 12, there are a few notable differences between the RV and COSMOS instruments.

Similarities and Differences of Terrestrial and Planetary CRNS.

Orientation.

In Figures 9, 11, and 12, note the orientation difference between the RV detectors (horizontal, to maximize the detection of neutrons directly below the instrument or rover) and the COSMOS detectors (vertical, to maximize the radial sensitivity, encapsulating an

entire agricultural field or land surface process, like a desert watershed). Until recently, this difference in configuration remained a purely hypothetical explanation.

Peplowski et al., 2023, studied the effect of increasing angle on the neutron count rate for a neutron spectrometer instrument much like the COSMOS and RV instruments. The primary differences between the NS instrument used here and the one used in Peplowski et al., 2023, are:

1. The use of a Cd thermal neutron shield (in place of the boronated thermal neutron shield on the RV detector) in Peplowski's work, though both thermal neutron shields achieve similar results.
2. The use of a AmBe neutron source in a lab setting (instead of GCRs in a field setting) by Peplowski, in other words this is active NS rather than passive.

Peplowski et al., 2023 took both thermal and epithermal detectors, set them adjacent to a moderator pool and increased the angle from horizontal to vertical in 15 degree increments (Figure 13).

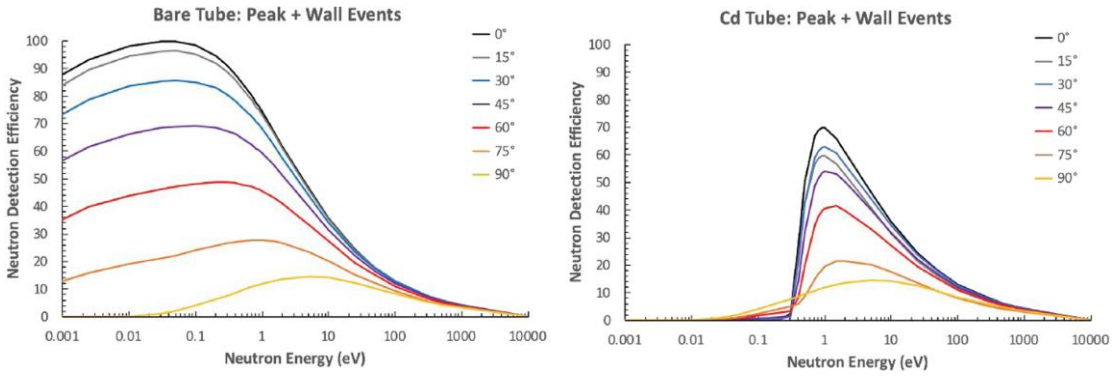

Figure 13. Orientation Results from Peplowski et al., 2023. The neutron efficiency from their bare tube (thermal neutrons), and their Cd tube (water sensitive domain; low-end of the epithermal neutrons, < fast neutrons due to the absence of a HDPE moderator) decreases as the angle increases.

The decrease in neutron detection efficiency correlates with an increase in angle (Figure 13), indicating that the pool of moderators takes up a smaller proportion of the FOV as the angle increases, and suggests that as the angle increases, so too does the radial sensitivity.

This implies that the logic behind the orientation of the COSMOS and RV units is likely correct.

Portability and Moderator Thickness.

As observed in Figure 11, the RV units are portable and approximately half the length of the COSMOS detectors (see COSMOS and RVs sections for precise measurements).

However, to compensate for the smaller length of the moderated detector in the RV units, additional layers of moderator are required to retain the sensitivity to the same range of neutron energies at a count rate high enough to allow the calculation of WEH that is within acceptable tolerances even after atmospheric corrections are applied.

The thickness of the moderation material (HDPE) with respect to the specific range of neutron energy measured has been studied in experiments with a set of detectors each surrounded by a sphere of moderating material of different thickness, also called a Bonner sphere or multisphere [Knoll, 2000; Goldhagen et al., 2002]. Multisphere measurements demonstrate that increasing the moderator thickness increases the neutron energy range the detectors measure, though it does not correlate in a linear fashion.

The RV moderated detector has four, ¼ inch sheets of HDPE (Figure 10), while the COSMOS moderated detector has only one, ¼ inch sheet.

Each sheet of HDPE weights approximately 1.45-1.85 kg (3.20-4.08 lbs). In total, the RV moderated detector weighs approximately 17.15 kg (37.82 lbs), compared to the RV bare detector which weighs 4.10 kg (9.04 lbs).

To increase the portability of the RV detector, removal of several sheets of HDPE will be considered and tested in the field.

Thermal and Epithermal Detector Uses.

In terrestrial hydrology, the bare detector has been used in subsurface detectors paired with a neutron source, because thermal neutrons have interacted with more moderators than higher energy neutrons [Rasche et al., 2023]. Zreda et al., 2012 states that "The fast (measured with the moderated detector) neutron data are used for measuring soil moisture while the thermal (from the unmoderated detector) neutron data are used for detecting and potentially quantifying water that is present above the land surface in snow, vegetation, etc.", though Zreda also notes that "fast" is used as a generalization to refer to both the fast and epithermal domains, as a way to denote that the moderated detector measures neutrons traveling at faster speeds than the bare detector.

When considering the neutron lethargies (Figure 2), and reviewing the energy ranges of neutrons as well as the kinetic energy equation, Zreda's hypothesis follows a simple logic: thermal neutrons that interact with water are traveling too slowly to emerge from the subsurface, and are more likely to be absorbed instead of elastically scattered out of the subsurface. This is considered having a short neutron attenuation length.

Similarly, on Earth, H_2O has some phases that are not common on rocky worlds without a thick atmosphere and a water cycle, for example: snow and rain. This work will primarily focus on water in liquid form, as that is the most common version on Earth. Snow as a surface water contributor has also been studied by terrestrial hydrologists who prefer to eliminate counts from snow via calculation of a Snow Water Equivalent (often abbv. SWE) using snow depth and density measurements, in order to remove surface H signal contributions from snow and still accurately calculate the SM content of the subsurface [Schattan et al., 2017; Tian et al., 2016; Schron et al., 2021; Weimar et al., 2020].

Ice on the surface, though it is more dense, would likely appear to have a similar effect on the neutron lethargies as snow, simply a higher WEH per volume (density). Understanding how ice or frost in the subsurface geochemistry (SM or LW) could contribute to the signals of both detectors individually, rather than a WEH signal focused on the volumetric wt % (or alternatively, density) of water in snow, ice, and liquid forms could greatly benefit analog neutron spectroscopy field work moving forward.

PNS signals from ice at the poles have been studied on Mars via an orbital detector onboard the Mars Odyssey known as the Gamma Ray Spectrometer (GRS) suite which includes the High-Energy Neutron Detector (HEND) instrument [Feldman, et al., 2002; Mitrofanov, et al., 2002]. We know there is ice at both poles of Mars, and we know that the north polar ice cap is primarily H_2O [Farmer et al., 1976; Kieffer et al., 1976; Carr, 2006] with a seasonal CO_2-ice cap above it [Feldman et al., 2002; Mitrofanov et al., 2002; Carr, 2006], and that the south polar ice cap is H_2O with a permanent CO_2-ice atop it [Byrne and Ingersoll, 2003; Carr, 2006]. HEND Results indicate that a high

concentration of subsurface H_2O-ice beneath CO_2-ice is indicated by an increase in thermal neutron energies [Feldman, et al., 2002], and a decrease in epithermal [Feldman, et al., 2002; Mitrofanov, et al., 2002] as well as a decrease in fast neutron energies [Mitrofanov, et al., 2002]. Interestingly, CO_2-ice overlaying a H-rich soil (not H_2O-ice) is indicated by an increase in thermal and epithermal [Feldman et al., 2002], and an unchanged level of fast energy neutrons [Mitrofanov et al., 2002]. It may be helpful to know that CO_2-ice (surface CO_2-ice) shows a consistent decrease in all three energies across the board [Feldman et al., 2002; Mitrofanov, et al., 2002], while CO_2-frost (similar to subsurface CO_2-ice) shows a decrease only in the thermal and epithermal ranges while the fast energies remain relatively constant [Mitrofanov, et al., 2002].

Moving down to the surface of Mars, the DAN instrument onboard Curiosity has one Cd wrapped ^{3}He proportional counter, and one bare. This leaves the Cd wrapped detector sensitive to the lower range of epithermal neutrons (< fast) and the bare detector sensitive to both thermal and the same range of epithermal neutrons [Czarnecki et al., 2020, 2023; Hardgrove et al., 2011; Litvak et al., 2014; Mitrofanov et al. 2012; Tate et al., 2018, 2019]. The count rates must be differenced in order to determine the thermal neutron sensitivity. Then a passive geochemical index can be produced from these readings [Tate et al., 2018, 2019].

Topography.

On Mars, topography has also been noted to influence the neutron count rate [Dibb et al., 2022, 2024; Berner et al., 2022, 2023, 2024]. This has also been considered as a potential contributor to signal for detectors on Earth [Schron et al., 2023; Hewitt et

al., 1976], indicating it is of relevance to vertically and horizontally oriented detectors. Therefore, all selected analog field sites were chosen with no significant topography and therefore minimal slope, if any, in mind to eliminate the need to correct for topography.

Methods and Results

Several field tests were conducted to confirm WEH sensitivity and calculation processes, determine detector radial sensitivity in various configurations, find ideal experimental moderator thickness with respect to portability, and sensitivity to vegetation of the RV instruments.

Vegetation Sensitivity Test.

As was demonstrated in Figure 3, neutrons that interact with the vegetation increase the signal from the water sensitive domain, and decrease the signal from the thermal domain before and after clear-felling a forested area [Vather et al., 2020]. Vather et al., 2020 saw an increase in raw epithermal counts of 12.43%, and a comparable decrease in thermal neutrons (though it was not quantified) after clear-felling the entire, forested FOV of their COSMOS CRNS.

Vegetation correction factors are typically reported as root mean square error of the count rate, which means the correction factors are specific to the instrument and GCR flux at the specific site and time [Baatz et al., 2015; Vather et al., 2020]. However, for planetary analog work, the development of a generalized correction factor based on several different instruments is more effective. Here, I will attempt to approximate a

general correction factor (a percentage) as a guide for analog PNS instruments with vegetation in the FOV of the detectors.

To confirm if this pattern is also seen in desert regions with sparse vegetation, we conducted a test in a residential region of Tempe, AZ before and after the removal of two citrus trees (one ~6.5 m diameter, and one ~2.5 m diameter trees when viewed on google earth). Considering the radius determined in the quantification test (~31 m in the horizontal, tripod configuration), the trees take up approximately 14.5% of the FOV. The water content of trees is estimated by cellulose ($C_6H_{10}O_5$) content, approximately 55.6% H_2O by weight, and is used as an approximation for dry, above-ground biomass (i.e. trees and other desert adapted vegetation) for CRNS functions [Vather et al., 2020].

We set up the RV instrument between two trees that were to be removed, for a several hour duration before removal, and repeated at the same coordinates after removal. When the trees were removed, the roots were left behind, and the detectors were returned to the same coordinates before the roots dried out. Therefore, the WEH of the tree is considered surface water, as opposed to subsurface water.

We determined that during our desert vegetation removal test, thermal count rates decreased by approximately 16%, while epithermal count rates increased by approximately 7% after tree removal (Figure 14).

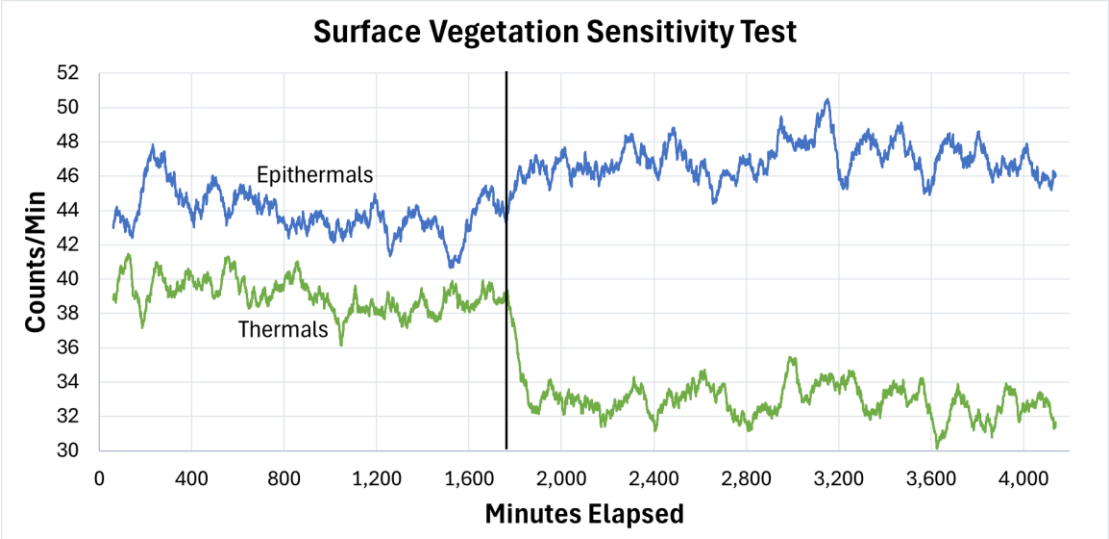

Figure 14. Vegetation Test Changes in Average Count Rate. This is the same dataset published in our 2024 abstract [Gonzales and Hardgrove, 2024b]. All data is shown as a 60-minute moving average to clearly show the trends. Epithermals are in blue, thermals in green. The vertical line indicates the time the trees were removed.

It would be easy to mistake the decrease in thermal counts after the tree removal (as seen in Figure 14) for an increase in concentrations of neutron absorbers. However, the increasing epithermal count could contradict that, but the small increase in epithermal counts could also be easily missed with shorter integration times. In order to prevent misidentification of either scenario, correcting for vegetation within the FOV of the detectors is advised.

Recall that Zreda et al., 2012 stated that the moderated detector is more sensitive to the subsurface SM, while the thermal detector is more sensitive to surface WEH like snow or vegetation. The larger decrease in the thermal neutron counts (~16%), compared to the increase in epithermal neutron counts (~7%) would suggest that Zreda is correct, however additional correlation with subsurface water would be needed to conclusively determine a correlation.

To more clearly show the changes in the four characteristic energy levels of a neutron lethargy plot, observe Figure 15, below, where the data has been reformatted as a bar chart approximation of the neutron lethargy spectrum. Thermal energy ranges are approximated by the average raw thermal neutron count rate. Epithermal energy ranges are approximated by the average calculated moderated neutron count rate after atmospheric corrections. Fast energy ranges are approximated by the average raw moderated neutron count rate. And the high-energy ranges are approximated by the solar flux (F_{SOL}), considered GCR intensity, multiplied by the average thermal energy count rate during the first segment of data collection at this field site in order to approximate increases and decreases in the intensity flux during the entirety of the test. All energy ranges are in units of counts per minute (cpm) which is used as a simple numerical model of signal intensity.

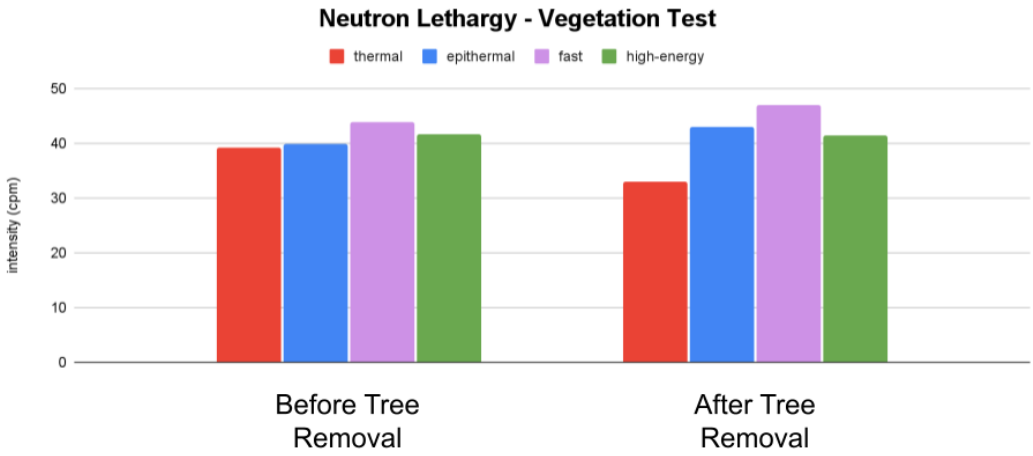

Figure 15. Neutron Lethargy Fluctuations Before and After Tree Removal. While the intensity of the incoming neutron flux did not change significantly, the thermal neutron counts decreased, and the epithermal and fast neutron counts increased after tree removal. Note that the difference between the epithermal and fast columns remains approximately the same before and after, indicating that the increase in both columns is from the tree

and not humidity. Recall that the increase in epithermal ranges indicates a decrease in WEH, confirming the WEH was primarily from the biomass itself and not groundwater.

In Figure 15, the diverging trend between the thermal (decreasing) and epithermal (increasing) count rates is a result of vegetation and not humidity or compositional change is more clearly demonstrated via the lethargy spectrum.

If future planetary field analog tests are conducted in regions with vegetation, correcting the diverging pattern with a ~10% decrease in the epithermal count rate, and a ~15% increase in the thermal count rate to help isolate the change in counts due to subsurface water abundance, particularly for sites along a traverse. Localized tests in regions with more and less vegetation depending on the region in use are recommended to determine a specific percentage for each site in order to make such adjustments

Regardless, vegetation can also be used as a proxy for high concentrations of H, C, and O in the topmost stratigraphic layer.

Radial Sensitivity Scale and WEH Confirmation Test.

As mentioned previously, the COSMOS radial sensitivity is on the order of hundreds of meters (~130-240 m [Andreasen et al., 2017; Kohli et al., 2015]). The RV units are approximately half the volume of the COSMOS units. However, radius does not scale directly with the volume of the detector.

The simplest way to test the radial sensitivity is to move from an area with a high concentration of moderators to one with a low concentration of moderators, for example: stepping incrementally away from a lake or a playa in a desert.

To determine if the radius of the RV unit is on the same scale (field scale, hundreds of meters) as that of the COSMOS detector, the RV instruments were setup adjacent to a COSMOS detector then stepped farther and farther away from the COSMOS along a traverse. Both RV units were set up adjacent to the COSMOS units at approximately 0 m for the first data point. Then, the RV detectors were moved northwards in 100 m increments every few hours (Figure 16).

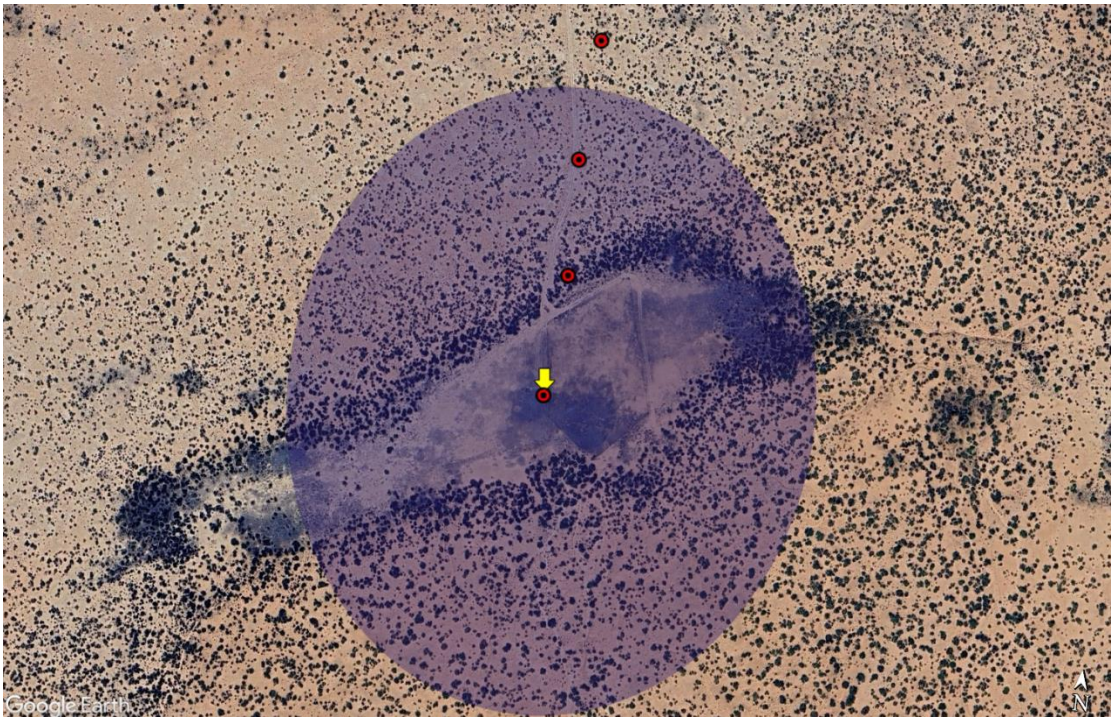

Figure 16. Map of the Small Playa Site. Measurements started adjacent to the COSMOS instrument (yellow arrow), then moved northward in 100 m increments (red dots), with respect to the COSMOS radius of sensitivity ~240 m (blue-shaded circle). Basemap is a Google Earth image. These data collection sites (red dots) will also be referred to as "stations". Recall that COSMOS is a stationary detector.

Data collected over several hours at each station is averaged to plot it with respect to distance (Figure 17), to portray the change in WEH stepping out of the playa. The data in Figure 17 has not been corrected for atmospherically emitted and moderated neutrons.

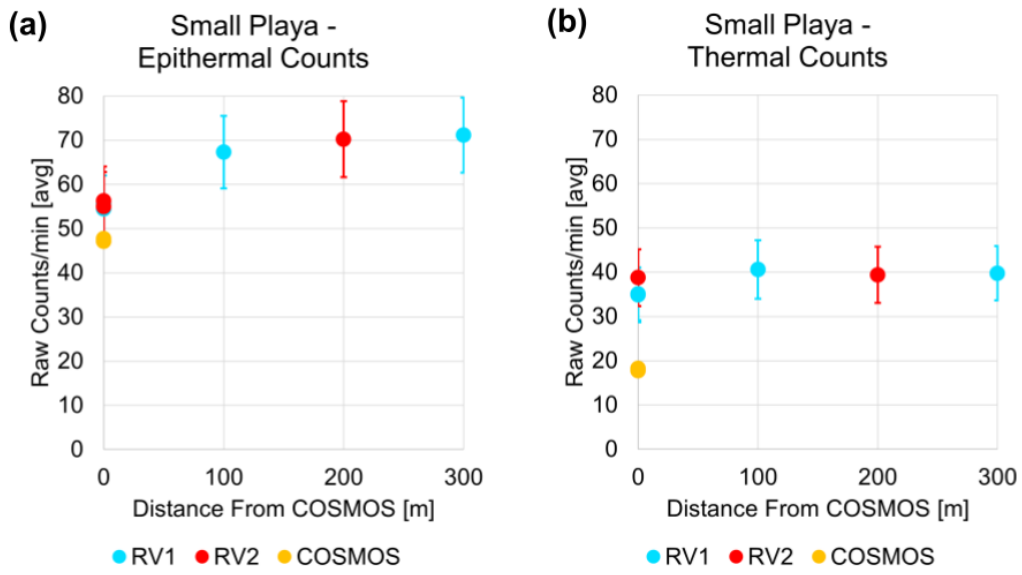

Figure 17. Averages of Raw Data Stepping Incrementally Outwards at the Small Playa. Note that the epithermal neutron counts (a) take on an exponential shape, while the thermal neutron counts (b) are nearly linear. Also note that the COSMOS counts are converted into cpm here and are lower than that of the RV detectors, a result of the different volumes and pressures of the detectors. Error is standard deviation of raw data.

Data from the moderated (epithermal) detector (Figure 17, a) takes on an exponential shape. The low neutron count rate in the interior of the playa indicates a higher concentration of WEH that dries out as the instruments are stepped out of the playa. This is supported by the presence of grasses that prefer wet conditions within the playa, framed by dense clusters of mesquite and creosote bush [Vivoni et al., 2021;

Schreiner-McGraw et al., 2016] that become sparser and randomly scattered in the arid, desert conditions external to the playa.

After atmospheric corrections are applied, the exponential shape of the moderated data curve becomes more muted (Figure 18).

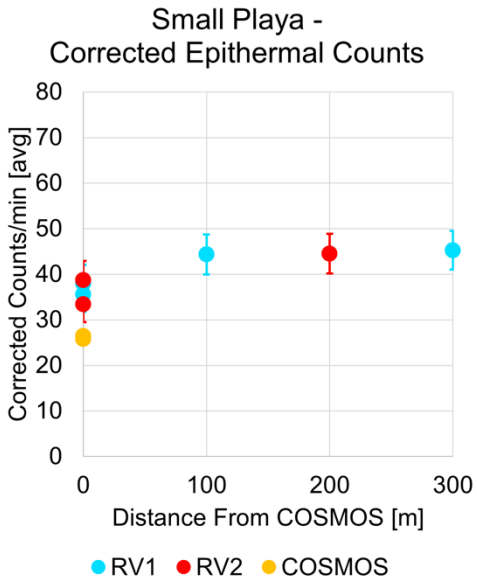

Figure 18. Corrected Neutron Count Rates Stepping Incrementally Outwards at the Small Playa. All count rates at this field site remain above the minimum limit found in Figure 5 (cpm < 15). Error is standard deviation of corrected calculations.

Once atmospheric corrections were applied, the WEH could be calculated from the RV epithermal measurements at each station using equation (8), see Figure 19, below. Note that WEH is inversely proportional to the neutron count rate.

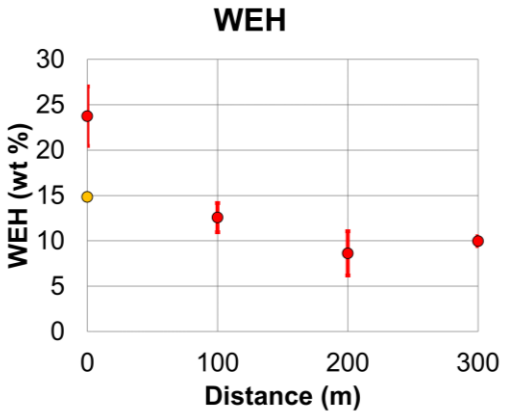

Figure 19. WEH for Each RV Station (red dots). Error bars show the standard deviation of the calculated WEH values for each station. COSMOS WEH is also calculated (yellow dot), though recall the 240 m maximum radius, a FOV that is approximately 50% playa, and 50% desert outside of the playa (Figures 16 and 20).

Recall that the COSMOS instruments are stationary, which allows for the assumption that the geochemistry remains constant during the calculation of SM weight percentages. In order to approximate the geochemistry in the equations, the COSMOS team collects samples within 200 m of the COSMOS detector, at approximately 18 different locations and spanning every 5 cms in depth, totaling 108 samples in all [Hurtado, 2024] (Figure 20).

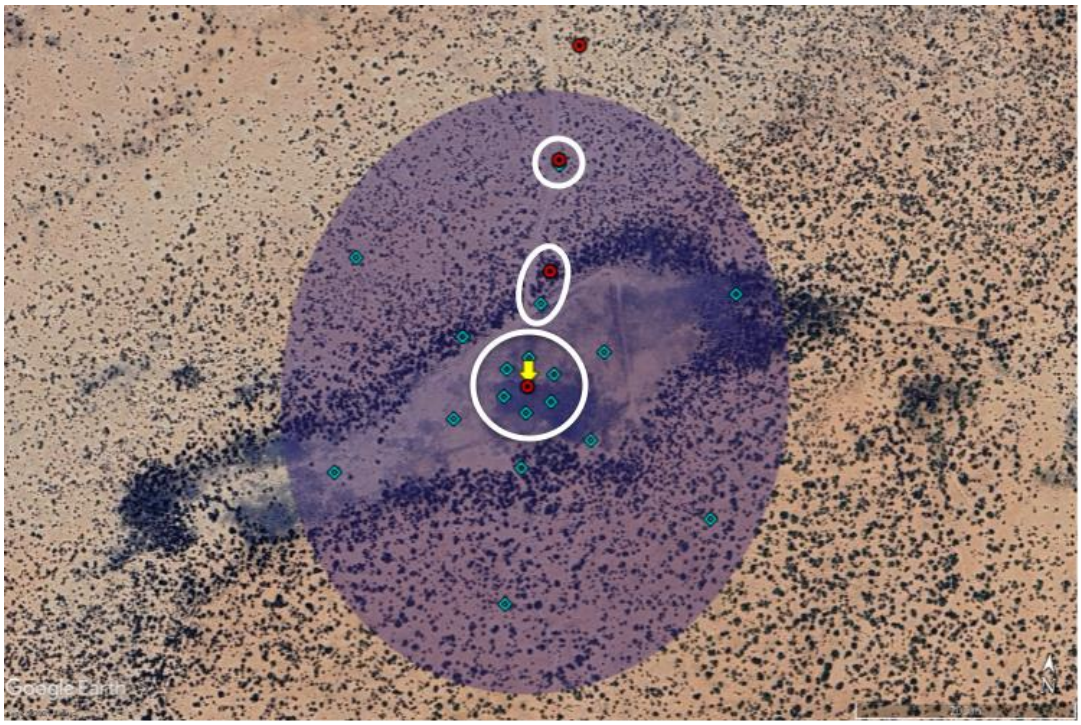

Figure 20. Sample Map of the Small Playa Site. The sampling coordinates (teal diamonds) from Hurtado et al., 2024 sit on top of the same map from Figure 16 (yellow arrow points to the location of COSMOS, blue region the COSMOS footprint, and the red dots are RV stations). Note that several of these sites are within a few meters of the RV stations along the RV traverse. Samples were collected at radii of: 25 m, 75 m, and 200 m. For each RV station, the closest sample(s) was used as ground truth (white circles). For the station closest to COSMOS, the samples along 25 m radius circle were averaged. For the 100 m station, the nearest 75 m sample was used. For the 200 m station, the nearest 200 m sample was used. Since no samples were collected beyond the 200 m station, the 300 m station was compared to the 200 m sample.

The samples collected at these locations were used to approximate the actual water content for these sites and confirm that the RV units have smaller radial sensitivities than the COSMOS detectors. WEH was also calculated from the COSMOS data during the same time interval.

COSMOS samples were collected a week prior to RV and COSMOS data collection, during the same weather conditions (a monsoon passed through the area

merely a few hours prior to sampling and data collection, and the playa was beginning to dry out during the 100 degree Fahrenheit day as the samples and RV data were collected moving radially outwards from the COSMOS site over periods of several hours), and used the WEH measurements from the samples at all 5 cm intervals (0 – 30 cm) for each coordinate. The sample WEH values at the sites closest to each RV station were used as ground truths (Figure 20).

WEH from the samples at varying depths with an average sample WEH at all depths were compared to the calculated WEH from the RV measurements at each station (Figure 21).

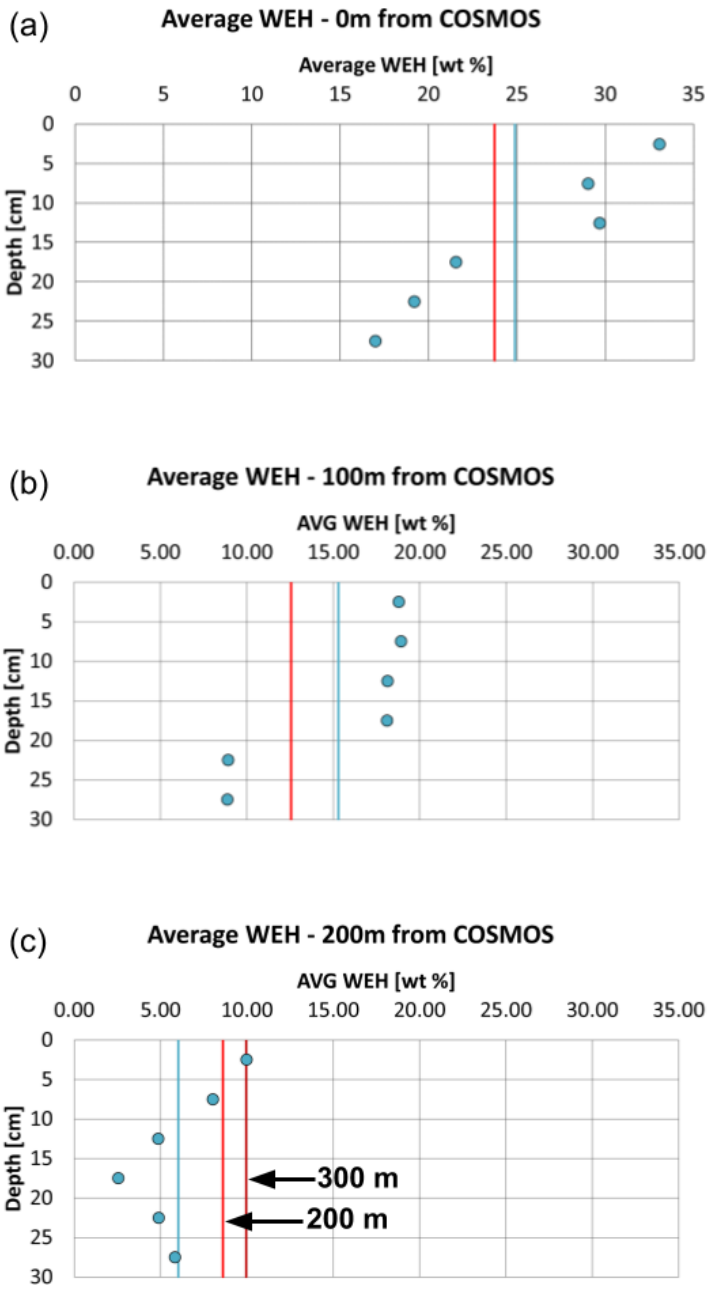

Figure 21. Sample-Measured WEH Compared to RV-Calculated WEH. Samples at 5 cm depth increments at each site show the change in water content within the top 30 cm of soil (teal dots). Averaged sample water content for 0-30 cm depths at each station are shown as a teal line. RV-calculated WEH are shown as red lines. Samples extend out to 200 m from the COSMOS detector, so the 300 m RV-calculated WEH (dark red line) is compared to the 200 m sample. Note that in all 3 plots there are two distinct layers within the top 30 cm. Note that the calculated WEH values assume a homogeneous, single layer reaching a depth of ~1 m. The correlation between the calculated WEH at 300 m and the 0-5 cm sample at 200 m could indicate that the 2-layers within 30 cm of the surface is no

longer present at 300 m. Standard deviation of the calculated WEH values for the RV units range from +/- 8.1 wt% (a), to +/- 2.8 wt% (b), to +/- 3.0 wt % for both 200 and 300 m in (c).

Observe how the WEH decreases as the RV units are stepped out of the playa (Figure 21). Also note that the average WEH for the 200 m and 300 m RV stations are within 3 wt % of each other in Figure 21, suggesting that the RV units are no longer detecting the hydration within the playa, also implied by the shallowing of the calculated WEH stepping out of the playa in Figure 16. Logically, it follows that the 200 and 300 m stations are both approximations of homogeneous desert, and have the same approximate water content.

The plots in Figure 21 demonstrate that the calculated WEH for each RV station is within one standard deviation of the average sample water content for each station, and thus within an acceptable margin of error. This suggests that the samples used for each station are within the FOV of the moderated detector, in other words, the RV radius of sensitivity is > 25 m. The shift of decreasing average WEH calculated for each RV station also suggests that the RV instrument at each station is no longer in view of the samples used at the previous station (with the exception of the 300 m station, where the 200 m samples are used as homogeneous desert ground truth from 200+ m), in other words, the RV radius of sensitivity is < 75 m.

To determine a more exact radial sensitivity, each detector will need to be considered individually. In other words, the data collected will need to be broken down into the four energy bins of the lethargy spectrum (Figure 22), using the same method as Figure 15 in the Vegetation Sensitivity Test section, above. Recall that variations in the

intensity (heights) of the four energy bins of the neutron lethargy spectra are the result of increases and decreases in the concentrations of moderators and absorbers present in the geochemistry.

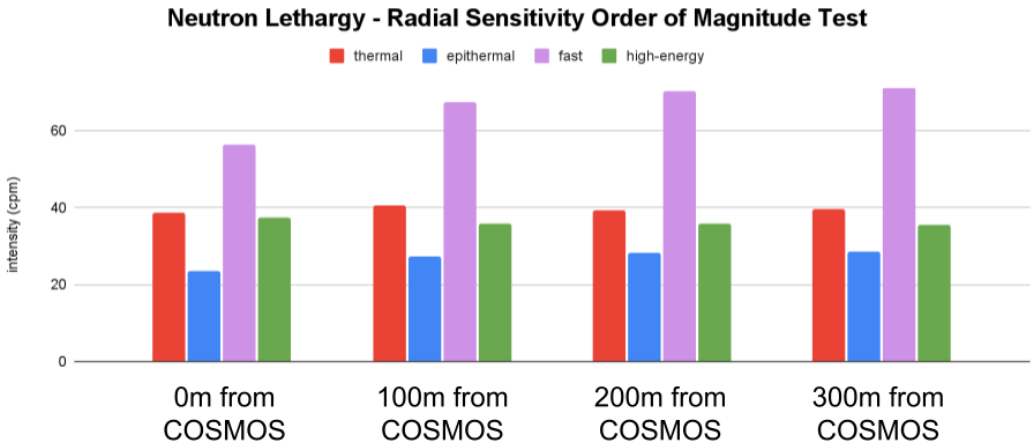

Figure 22. Neutron Lethargy Spectra for Radial Sensitivity Order of Magnitude Test at the Small Playa. Note that as the detectors are stepped out of the playa, the moderated count rates for both the epithermal and fast energy ranges increase, but that the majority of the increase is accounted for by the atmosphere peak. This is due to the fact that a storm had just passed through the area prior to data collection, and the warm summer weather caused the rain to evaporate. The relative humidity measured by the RV detectors increase from ~24% humidity during the first interval at 0 m, to ~34% during the other three intervals. Also recall that the increase in the epithermal water sensitive domain indicates a decrease in the WEH (Figure 2, d-f), which is present at all four distance increments, though it is lower than the increasing humidity.

Interestingly, in Figures 17, 18, and 22, there is a slight increase in thermal neutrons at the 100 m station, which corresponds to a decrease in the high-energy domain. This would suggest that there are either fewer neutron absorbers in this zone at the edge of the playa, despite the decreasing neutron intensity from GCRs, or there is an increased amount of vegetation within the FOV. Note the clustered mesquite and creosote

bushes in the maps in Figures 16 and 24, indicating that the most likely cause of the diverging trend is the presence of vegetation.

In Figures 19, 21, and 22 the RV-calculated WEH indicates a smaller footprint than the COSMOS detector (~240 m). The RV footprint is > 25 m, and < 75 m, thus likely ~50 m, approximately one order of magnitude less than that of the COSMOS detector.

The next step is quantifying the actual radial sensitivity of the RV instruments.

Radial Sensitivity Quantification Test.

The smaller the change in WEH, the harder it will be to measure the radial sensitivity; thus, the small playa was a less satisfactory site. We selected Fireman's Cove at Lake Pleasant, AZ to quantify the radius of sensitivity.

Measurements started on a small peninsula (considered "over the water" or "surrounded by water" and thus the majority of the FOV is filled with moderators) and moved towards shoreline, and then away from the water first in small increments (2-3 m increments) until ~10 m past the shoreline, where increments increased to 5 m. Cart and vertical configurations were collected simultaneously, tripod configuration was collected two weeks later, when the water level had risen ~1 m.

This was tested in three different detector configurations (see Figure 12):

1. horizontally, on a cart, ~0.5 m off the ground
2. horizontally, on tripods, ~1 m off the ground
3. vertically, center of gravity ~30 cm off the ground

Tripod configuration repeated roughly the same test and added one additional point at the 55 m distance, but did not include the peninsula as this test was conducted approximately two weeks later and the water level had risen, leaving the peninsula underwater (see Figure 23).

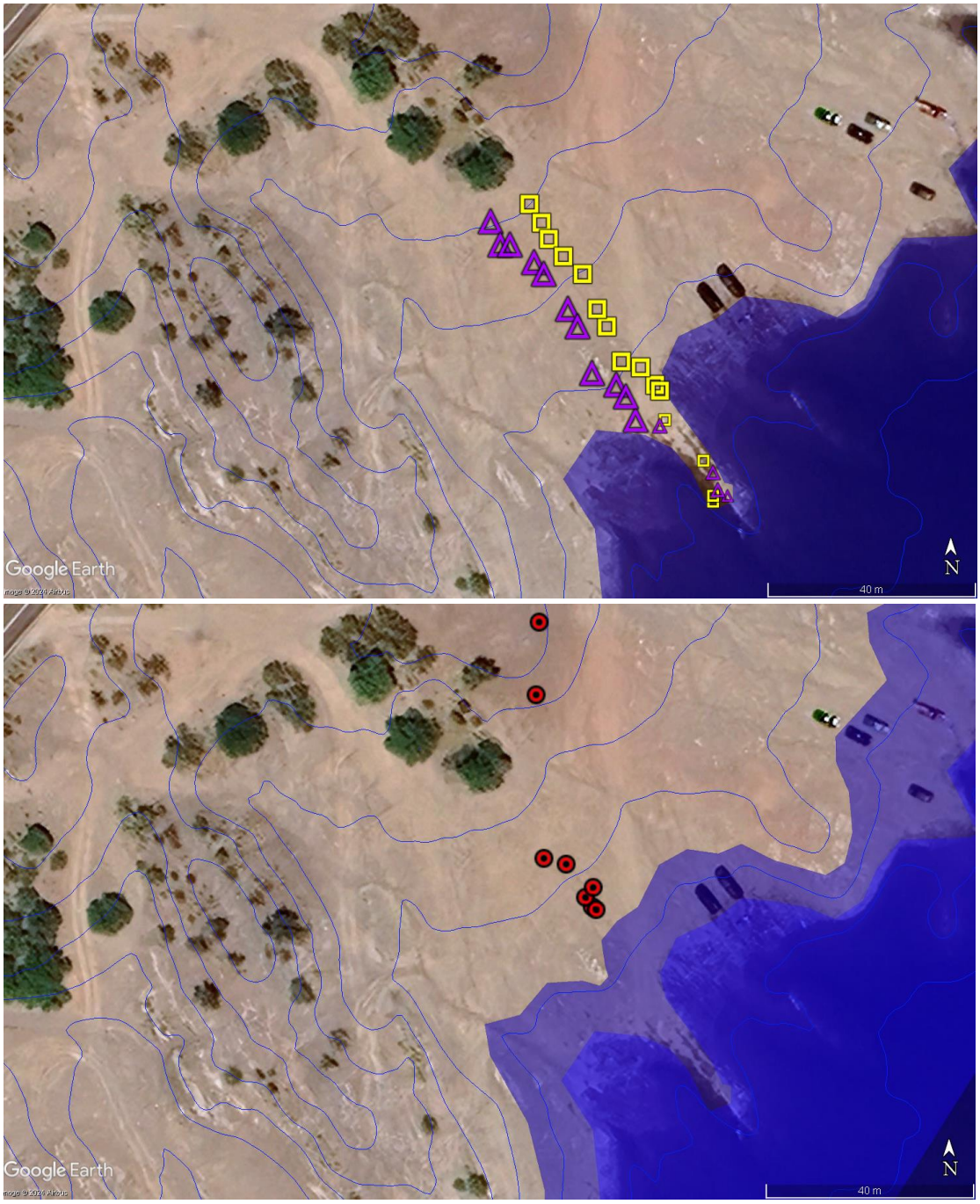

Figure 23. Maps of Fireman's Cove at Lake Pleasant. Blue polygons represent approximate lake fill levels, or shoreline, at the time of data collection. Blue lines show the local topography in 1 m contour intervals [derived from USGS 2021 survey via OpenTopography] overlaid on a global Google Earth satellite map. Top image shows coordinates for cart-mounted sites (purple triangles) and vertically oriented sites (yellow squares), note the peninsula sites which will, from here on, be considered negative distances to shoreline. Bottom image shows higher lake levels and locations of horizontal

tripod-mounted sites (red dots). Note that the farthest coordinate from the water in the tripod configuration is the only location with outcroppings of rocks (not visible in the satellite imagery), potentially resulting in a compositional change at that site: data from that point will be included in plots but left out of calculations.

We also collected data over the water on a kayak, however, the kayak was made of polyethylene, and thus moderated both detectors, with the exception of the data at shore island, where the detectors were removed from the boat and set directly on the ground ~1 m from shore for ~30 minutes (see Figure 24).

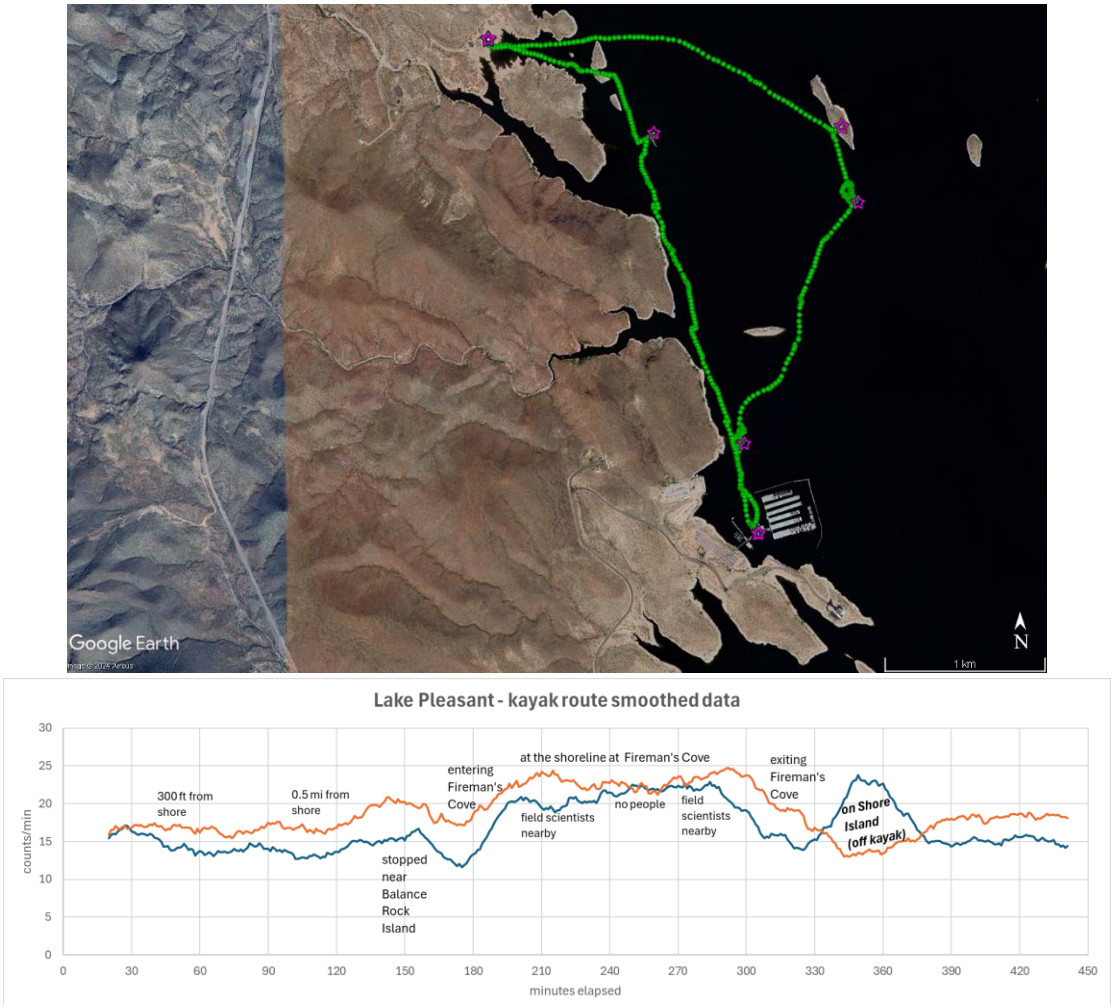

Figure 24. Lake Pleasant Kayak Route and Data Collected. In the top image, the dotted green line shows the route the kayak took around the lake, pink stars indicate sites where the kayak was kept in place for ~30-minute intervals, considered waypoints. The bottom image shows data from both the bare (orange) and moderated (blue) detectors. Notes in the plot indicate waypoints or point out changes that occur as the kayak approaches waypoints. Note that the moderated and bare detector data follow roughly the same trends, except during the excursion on shore island, where the detectors were removed from the kayak and placed directly on the ground. This is the only point at which the bare detector data behaves as expected. During the rest of the kayak data the kayak acts as an additional moderator to half of the instrument and changing the energy level of neutrons interacting with the bare detector. While on the kayak, the differences in the two lines could potentially be the result of different effects on the unmoderated half of the bare detector and the moderated detector from nearby topography.

Terrestrial hydrologists utilize a statistics method to calculate the approximate radial sensitivity of the moderated detector, explained in the Background Radial Sensitivity Section and summarized in equation (10). This will be calculated for the typical orientation used in all experiments listed herein (tripod-mounted horizontal) first, via the data collected at the lake, specifically for the moderated detector as seen in Figure 25 (green). This method fits an exponential curve to the data (black curves) and approximates the maximum cpm detected farthest from the concentration of moderators where it has stabilized into an approximately horizontal trend (~33 cpm; recall that we are ignoring the potential compositional change at the tripod site farthest from the lake), and the minimum cpm when the detector is over or at the nearest point to the water (~25 cpm). Subtract the minimum from the maximum, multiply the difference by 86%, and add the result back to the minimum to determine where along the curve the 86% lies, the resultant count rate (31.88, ~32 cpm, dashed grey line). Trace straight down from where the curve hits 32 cpm (dashed grey line), to determine the radius, in this case, ~31 m (Figure 25). Using the same process (lower black exponential curve in Figure 25; maximum ~30 cpm; minimum ~24 cpm), the radius of sensitivity when the detector is in the cart configuration (~30 cm off the ground) is ~24 m.

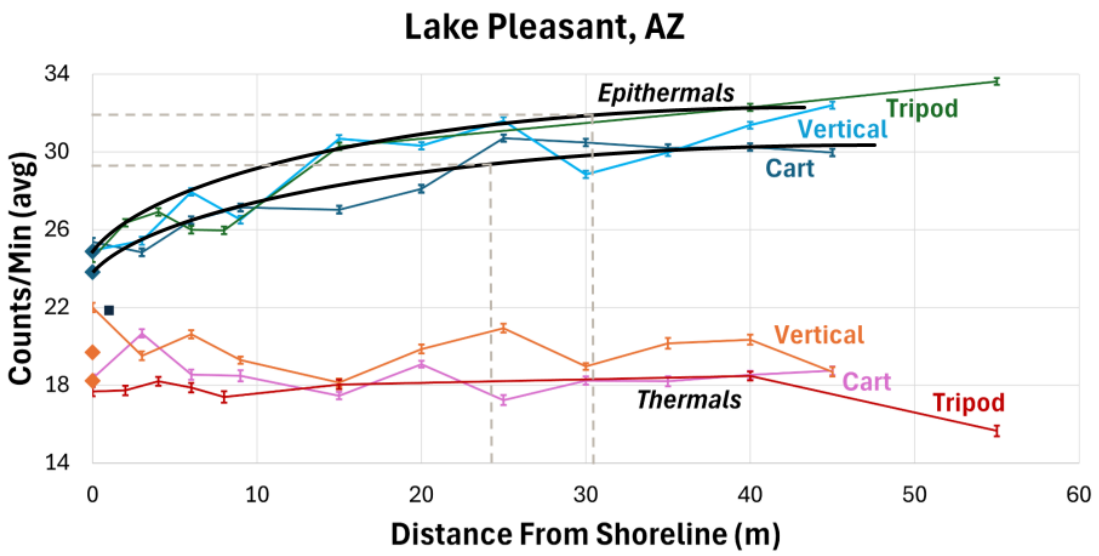

Figure 25. Data Collected at Fireman's Cove. Epithermal data is shown in cool colors (blue, teal, green), thermal data is in warm colors (orange, red, pink). Instrument configurations are noted in the same color as the corresponding lines. Note that this includes the singular data points collected on shore island where the detectors were set directly on the ground, accessed by kayak for both thermal and epithermal (squares), as well as the average of the data collected on the peninsula in vertical and cart configurations (diamonds). The same 86% method cannot be used for the radial sensitivity of the bare detector, as the data cannot be fitted to an exponential curve (black curves and grey dashed lines). Observe the diverging trend in the data points collected farthest from shore (55 m), matching the trend seen during the vegetation test. While there was nearby vegetation (see map in Figure 23), the 45 m data was also collected near larger vegetation and does not appear to follow the expected trend. Outcrops of basaltic tuff were observed within the vicinity of the detector at the 55 m site, which could indicate higher concentrations of neutron absorbers. As data at this increment appears to have been an outlier in the dataset, it was not included when fitting the tripod data to an exponential curve.

Note that in the epithermal data in Figure 25, the vertical and tripod configurations fit roughly the same exponential curve (teal and green, respectively), while the cart configuration is notably lower (dark blue). Recall that in the orientations seen in Figure 12, the center of gravity of the detector sits approximately:

~30 cm off the ground for the horizontal cart configuration,

~1 m off the ground for the horizontal tripod configuration, and

~50 cm off the ground for the vertical orientation.

In Figure 25, the average epithermal count rate at all increments for the tripod configuration (c) are higher than that of the cart (a). Both tripod and cart configurations keep the detectors in horizontal orientations. This suggests that the increase in epithermal neutron signal is likely because of the increased distance between the ground and the detector. Both configuration curves in Figure 25 are also higher than data points from when the detectors were set directly on the ground at shore island (squares), producing radii of ~31 m and ~24 m, respectively. This indicates that the increasing distance from the surface has a similar effect to changing the angle of the detectors.

Also in Figure 25, the epithermal data display the expected curve, while the thermal data does not. This suggests that the radial sensitivity of the two detectors is different. It is possible that the radius of the thermal detector is significantly smaller than that of the epithermal detector. Thermal neutrons have a short attenuation length, due to the slow speed allowing the neutrons to be absorbed quickly rather than continually elastically scattered, which supports the likelihood of a smaller radius for the thermal (bare) detector. It is also plausible that the high WEH of the lake itself could bear more resemblance to subsurface WEH rather than surface WEH, which could be the reason the thermal signal hardly changes in the presence of the lake but was more significantly affected by the presence of vegetation. Though, the relationship between surface and subsurface WEH with respect to the lake will require more comparisons with other moderator and absorber pools to untangle.

The decreasing trend in the thermal data between 0 and 16 m from shoreline in the vertical and cart configurations could be the result of stepping away from the water, however, during the data collection many cars moved into and out of the FOV, suggesting that the high amount of variation in the thermal data could also be the result of the high concentration of plastic and gasoline and iron in a car taking up a large portion of the FOV. The American Chemistry Council estimates that the average car is approximately 50% plastic by weight. Ignoring the gasoline (though it is a WEH contributor) due to its unpredictable variability, as well as the iron and other heavy metals (neutron absorbers), we can estimate the WEH of a car based purely on the plastic content. Approximating the size of a typical car based on the average parking space, ~8 feet by ~19 feet (rounded to the nearest foot) according to the city of Phoenix parking regulations, then converted into a circular area in meters gives us ~2.12 m radius approximating a typical large car. If, for argument's sake, the radius of sensitivity of the bare detector is ~20 m, one car fills > 10% of the FOV with at least 50% WEH. According to the vegetation sensitivity test results a 55.6% WEH occupying ~14.5% of the FOV creates a noticeable change in the neutron count rate. Decreasing both the area and WEH content by 5% retains proportionality, therefore a car is likely able to affect the data and would bear resemblance to vegetation when within the FOV. There is a significantly higher amount of variation within the thermal neutron count rates compared to the epithermal count rates as seen in Figure 25, indicating that the activity near the instrument has a larger effect on the thermal data than the epithermal data. During all lake tests, many cars and kayaks (lots of HDPE and other hydrocarbons) were present and moving through the entirety of Fireman’s Cove, many of which were within 20m of both

detectors for various periods of time. Therefore, it can be argued that the radial sensitivity of the bare detector is < 20 m.

The vegetation test also indicated that a high concentration of surface WEH created a diverging trend in the epithermal and thermal datasets.

If we use a modified version of the 86% method on the bare detector data (exponential shape curves down instead of up, all other math remains the same), as well as the concept that the vertical orientation likely has the largest FOV (the water fills a larger percentage of the FOV at shoreline, but cars add too much variability farther from the lake), and follow the diverging pattern in thermal and epithermal neutron counts seen in the vegetation test (exponential shape curves down instead of up, indicating that the lake could be considered surface water), then we can estimate a rough radial sensitivity (lowermost black curve in Figure 26). The highest count for the vertical orientation is at shoreline, ~22 cpm. If the vertical orientation has a larger radius, following the logic of the COSMOS detectors, then the FOV of the vertical instrument farther from the lake may include too many cars to be a good approximation of the actual WEH of the subsurface. However, the cart and tripod thermal data show a consistent flattening trend farther from the lake, producing a consistent minimum of ~18 cpm. Using the same math, this produces a maximum radius at ~21.44 cpm, of ~2 m (Figure 26).

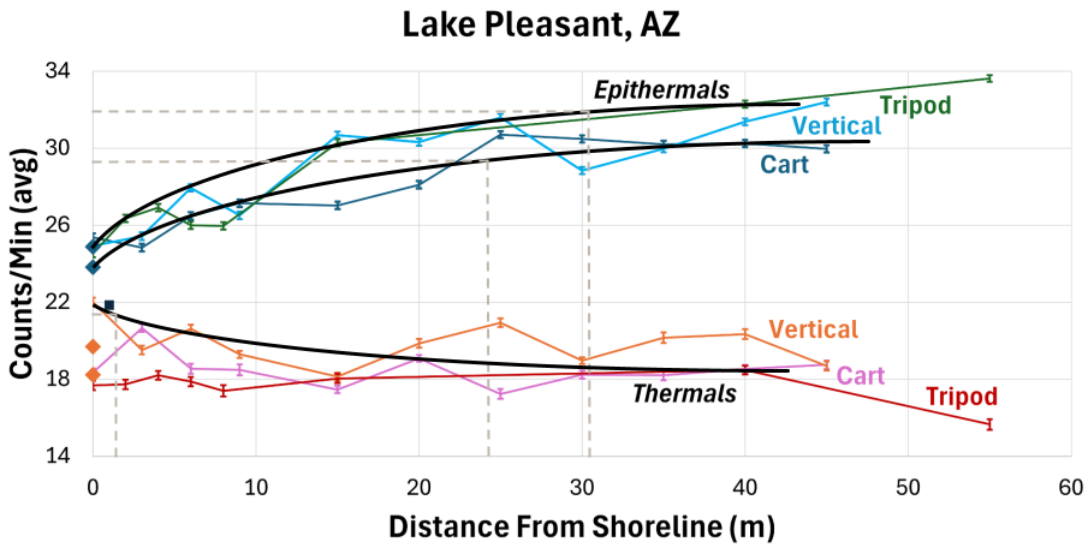

Figure 26. Modifying the 86% Method for the Bare Detector. The modified version of the same statistical method using an inverted exponential curve, while maintaining the remaining mathematical properties produces ~2 m radius for the thermal detector, regardless of configuration. The majority (86%) of the neutrons are emanating from within the radius, but anything with a very high WEH (i.e.: > 50% WEH with a large area, like a car) within ~20 m of the detectors could create an anomalous count rate in the data. In other words, anything farther than 2 m but closer than ~20 m is more likely to be seen in the vertical orientation (if the assumptions about orientation are correct).

The differences between the radii of the thermal and epithermal detectors indicates the importance of geochemistry when considering what each detector is measuring, both independently and with respect to each other. Usually, when considering composition, it is important to visualize the entire lethargy spectrum.

Changes in all four neutron energy bins are more clearly shown in a neutron lethargy approximation (Figure 27).

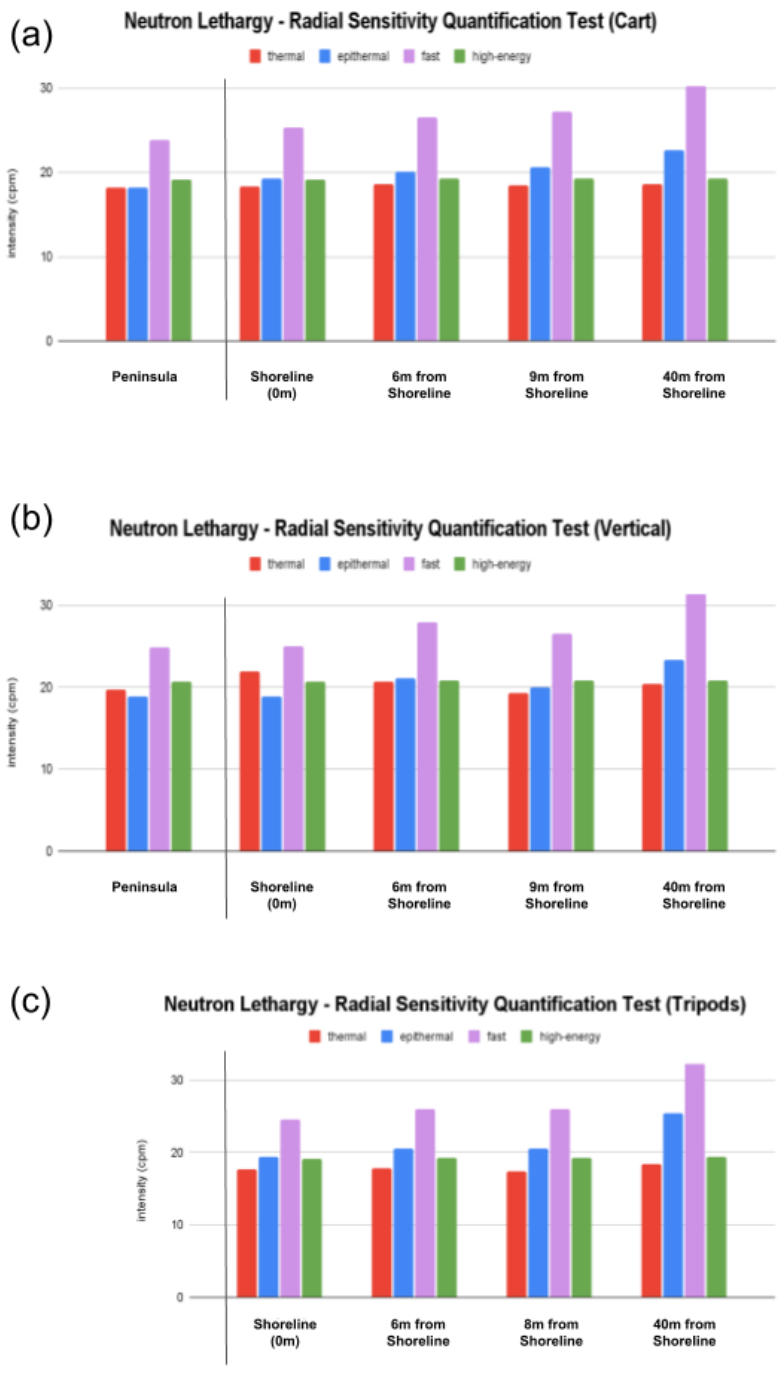

Figure 27. Incremental Neutron Lethargy Plots for Each Orientation at Fireman's Cove. The intervals chosen are not the same as the ones depicted in Figures 23, 25, and 26. Only the distance increments collected during both field excursions are used here. Note the increasing epithermal ranges moving away from the lake, indicating the decreasing WEH concentrations. As the height difference between the epithermal and fast energy bins remain the same during all data collection segments, the increase in the fast column

is not from humidity, but from the water content of the ground itself and therefore seen in both the epithermal and fast energy bins.

Figure 26 (radii) and Figure 27 (lethargy spectra) indicate that the thermal neutron counts (from the bare detector) are not as sensitive to the water in Earth conditions, when compared to the water sensitive domain (moderated detector). Though, in Figure 26 (radii), the farthest point from the water (at the location with a potentially different composition), has a lower thermal count rate. The epithermal count also goes up, suggesting this could be the result of the sparse desert vegetation. The nearby vegetation seen in the maps in Figure 23 (identified as Palo Verde trees by the Seek app by iNaturalist, 2024), however, the tripod point at 40 m is also close to the same vegetation (see map in Figure 23, b), and does not display the same diverging trend that would indicate plant biomass was the culprit. The plants are not within a 2 m radius, therefore the signal from the plants is not a likely contributor to the thermal neutron signal as much as it would contribute to the epithermal neutron signal. However, rock outcrops in the region near the farthest point from shore appeared a light purple in color, with randomly distributed vesicles ranging from a few mm across to ~0.5 cm maximum, likely a vesicular, basaltic tuff. Basaltic compositions could indicate higher compositions of Fe and Mg, both of which are more likely to absorb neutrons than elastically scatter them. Whether the diverging trend at this point is the result of a subsurface compositional change or vegetation is unclear, however, it does suggest that the best way to determine the radius of sensitivity of the bare detector is to repeat the same process replacing the large pool of water with a large pool of thermal neutron absorbers, like a basalt with a high-iron content.

The radius of sensitivity of the bare detector is also likely significantly lower on Earth than on other planetary bodies due to the observably low count rate at Earth's surface (seen in both epithermal and thermal detectors) indicating thermal neutrons that manage to elastically scatter out of the subsurface are often absorbed in the atmosphere before reaching the bare detector. This is known as a short attenuation length.

Despite the short attenuation length, we now have a radius of sensitivity for the thermal detector with respect to a large pool of moderators. It can also be concluded that moving the detectors farther from the ground, while retaining the horizontal orientation, increases the radius of sensitivity for the epithermal detector.

It also indicates that if changing the height of the detector by < 1 m can change the radius by ~7 m for the moderated detector and aid in the calculation of a radius for the bare detector, then it is likely that a change in orientation will also affect the radial sensitivity.

Orientation Test.

Recall the distinction between the orientations of the RV and COSMOS instruments and the assumptions about radial sensitivity inferred from both (horizontal has a smaller radial sensitivity, vertical a larger radial sensitivity) [T. Franz, personal communication, June, 2023], as well as the Peplowski et al., 2023 study of increasing angle on the neutron signal.

To confirm these assumptions about the orientations of the terrestrial and planetary instruments, while conducting the radial sensitivity test at Fireman's Cove at Lake Pleasant, one of the detectors was set in the vertical orientation (yellow squares on

the map in Figure 23; the light blue and orange in Figure 26, radii; Figure 27, lethargy spectra, part b).

In Figures 25 and 26, the epithermal horizontal tripod data (green) and the epithermal vertical data (teal) can be fitted to the same exponential curve. Despite the increase distance between the detector center of gravity and the ground in the tripod orientation, the vertical data has approximately the same resultant radius. Moving the moderated detector farther from the surface or changing the orientation of the detector increases the radial sensitivity, confirming the orientation hypotheses used in both terrestrial and planetary neutron spectroscopy.

An orientation test was also conducted at the Small Playa site in Jornada, NM (Figure 28), though the Jornada orientation test was conducted during a rainstorm, indicating elevated levels of surface water.

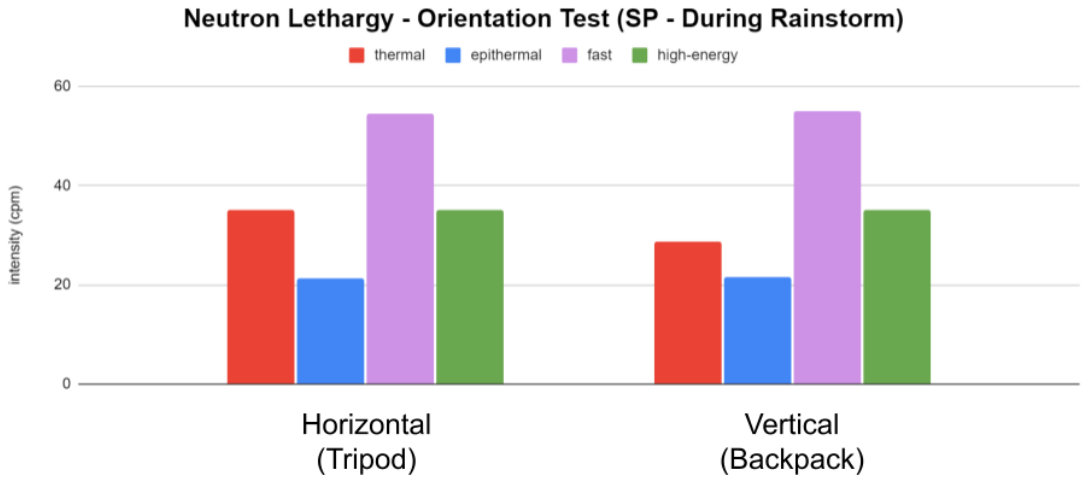

Figure 28. Neutron Lethargy Spectra for the Small Playa (SP) Orientation Test. While This test was conducted during a rainstorm, indicating it is actually testing two variables: orientation effects on neutron lethargy spectra and increased presence of surface water. Both datasets were collected simultaneously with both detectors < 2 m from each other, therefore GCR flux, geochemistry, and humidity are constants.

For the orientation test at the Small Playa, both RV instruments were setup adjacent to the COSMOS detector (all three instruments were < 2 m from each other), though the COSMOS data is not considered in this test due to the difference in detector volume.

Data in vertical (tripod-assisted vertical) and horizontal (tripod-mounted horizontal) was collected simultaneously. Therefore, geochemistry and humidity are constants. Data was collected over a span of several hours, but has been averaged over the entire time span, so time is not a factor. This means there is no environmental change from one lethargy spectrum to the next (humidity is constant, as is the presence of surface water).

In Figure 28, the only energy bin that varies between the two orientations is the thermal bin. This indicates that the thermal energy bin is sensitive to water at the surface, because that is what it is primarily measuring here.

Recall that the small playa appears uniform within the maximum FOV of the moderated detector (31 m), and that the average WEH from the samples collected in a 25 m radius circle from the COSMOS coordinate confirmed that the RV epithermal data could be used to accurately calculate WEH. Therefore, the geochemistry and WEH within the FOV of the detectors, averaged over the entire data collection period, can also be considered a constant. The only factor that is changing is the radius of the detector.

If the vertical orientation does have a larger radius, then the puddles of water collecting at the surface form a smaller surface layer, percentage wise, within that larger radius.

This both supports the Zreda hypothesis that the thermal detector is more sensitive to surface water than subsurface water, and supports the increasing radii hypothesis behind the orientations of PNSs in both planetary science and terrestrial hydrology.

Therefore, the maximum radius of sensitivity of the moderated detector in dry conditions is ~31 m in the horizontal tripod orientation, as well as the vertical orientation, and decreases the closer to the ground the detectors are placed (~24 m in the cart configuration). Similarly, the maximum radius of sensitivity for the bare detector is < 25 m, and likely ~2 m, though continued work repeating this radial sensitivity test with a body of high iron content instead of a body of high WEH content is recommended.

For all other tests conducted herein, the detectors were kept in the horizontal orientation and set up on tripods, to maintain consistency with planetary PNSs.

Now that both terrestrial hydrologists and planetary scientists are considering the applications of portable PNS instruments on Earth, orientation determines the mode of transport (vertically when attached to a backpack system, or horizontally when mounted to a roving system like the Curiosity rover), but weight is also important.

Moderator Thickness Test.

The moderated detector weighs 14.7 kg (32.4 lbs). The current setup has four sheets of ¼ inch HDPE (Figure 10), each weighing approximately 1.683 kg (3.71 lbs). It

also contains one sheet of non-removable boron shielding, weighing approximately 2.13 kg (4.7 lbs).

To increase the portability of the detectors, an additional test was conducted while in Jornada, NM. For this test, one RV unit was stationed approximately 25 m from the COSMOS detector, and remained there for the duration of the test (Figure 29).

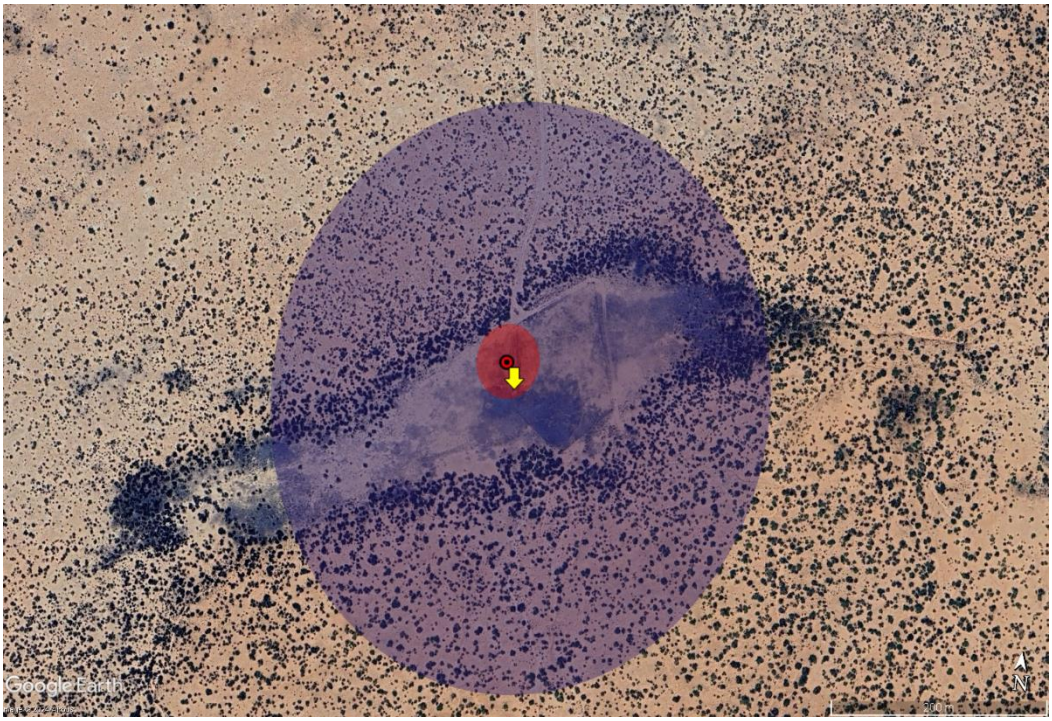

Figure 29. Map of the Moderator Thickness Test. Location of the RV detector (red dot) and footprint (horizontal tripod configuration; red-tinted circle) with respect to the COSMOS instrument (yellow arrow), and COSMOS FOV (blue-tinted circle), at the small playa field site in Jornada, NM. The RV unit is approximately 25 m from the COSMOS detector.

During the test, sheets (layers) of moderator were removed from the moderated detector, one at a time, every few hours (Figure 30).

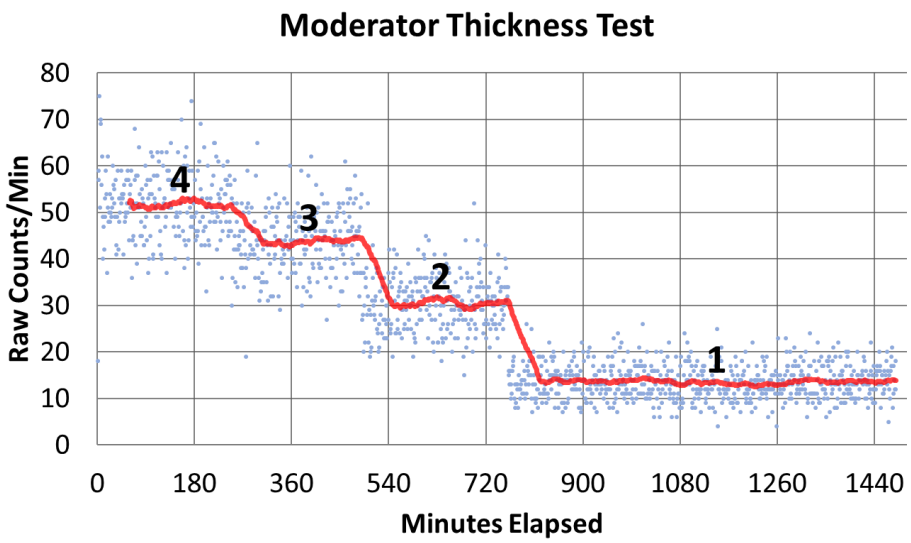

Figure 30. The Raw Data from the Moderator Thickness Test. Raw data is shown as blue dots, and the moving average using a 60-minute period is depicted as a red line. We began the test with all four sheets of moderator installed in the detector, then removed them one by one. As each sheet is removed, the moving average decreases. Atmospheric corrections have not been applied to the data at this stage, this is raw data. Variation in the raw data (blue dots) is due to natural variation in the GCR flux at the surface of the planet.

Comparing the average count rates per sheet seen in Figure 30 with the minimum count rate cutoff from Figure 5 (15 cpm) indicates that the counts from 1 sheet of HDPE are too low to calculate an accurate WEH.

Once the atmospheric corrections are applied, the counts from neutrons generated and moderated above the surface are removed, and the adjusted count rates can be examined.

WEH was then calculated from the raw moderated (epithermal) data using the terrestrial hydrology atmospheric corrections and the terrestrial WEH equation (8) for both the RV units and the COSMOS.

WEH from the COSMOS sample data (obtained in December of 2021 when conditions were comparable to those during the moderator thickness test) were used as ground truths (see Figure 31).

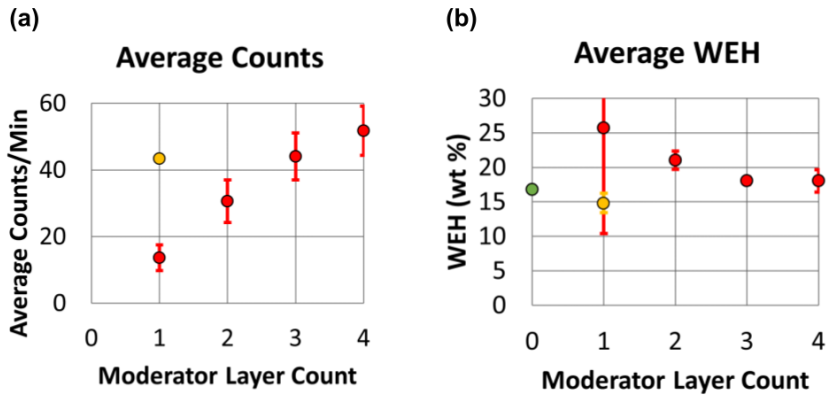

Figure 31. Average Raw Counts (a) and Average WEH Calculations (b) for Each Moderator Thickness. Yellow dots indicate COSMOS data with units of counts per minute and comparable thickness of the COSMOS moderator on plot (a); and the COSMOS-calculated WEH and COSMOS sample value of WEH. Note that the sample was obtained in December of 2021, during comparable conditions to those experienced during the moderator thickness test, but may show some variation. Error on both plots are the standard deviation of the data-collected and WEH-calculated for each thickness interval. Atmospheric corrections have not been applied to these averages of the raw count rates. Error is standard deviation.

Recall that the COSMOS detectors are roughly twice the size of the RV detectors to compensate for the low neutron flux at Earth's surface. To compensate for the smaller size of the RV unit and to increase the count rate enough to allow for accurate WEH calculations (> 15 cpm) from the boron-wrapped detector, the RV moderated detector has a thicker moderator.

As can be seen in Figure 31 (a), using the COSMOS as a control, the count rate of COSMOS (which only needs one ¼ in sheet of moderator due to the larger instrument size) is most comparable to the RV detector with three layers of moderator, rather than four.

Corrected neutron count rates from tests with only one and two sheets of moderator fall below the minimum cutoff (<15 cpm).

The average WEH calculated for each moderator thickness in Figure 31 (b), indicates that one layer is too thin for the reduced size of the RV detectors due to the large uncertainty in error and the count rate approaching the minimum limit rate of ~15 cpm before atmospheric corrections were applied (see Figure 5). WEH calculated from the one- and two-layer thicknesses indicate that the WEH is also overestimated, potentially due to the lower count rates causing the atmosphere correction factors to underestimate the amount of neutrons in the FOV of the smaller detectors. Recall that the average corrected count rates for the one- and two-layer thicknesses fall below the asymptotic cutoff (<15 cpm), confirming this. Also note the larger error bars on WEH calculated with 4-sheets. This could indicate that the amount of neutrons emitted and moderated in the atmosphere is overestimated, causing a higher error in WEH calculations (though an anomalously high WEH is not visible in the standard deviation of the data as the root cause is instrumentation error not calculation error).

To better illustrate the effect the moderator thickness has on the detection capabilities of the moderated detector, consider the above data as a factor of intensity. In Figure 32, the moderator thickness data has been reformatted as a bar chart approximation of the neutron lethargy spectra.

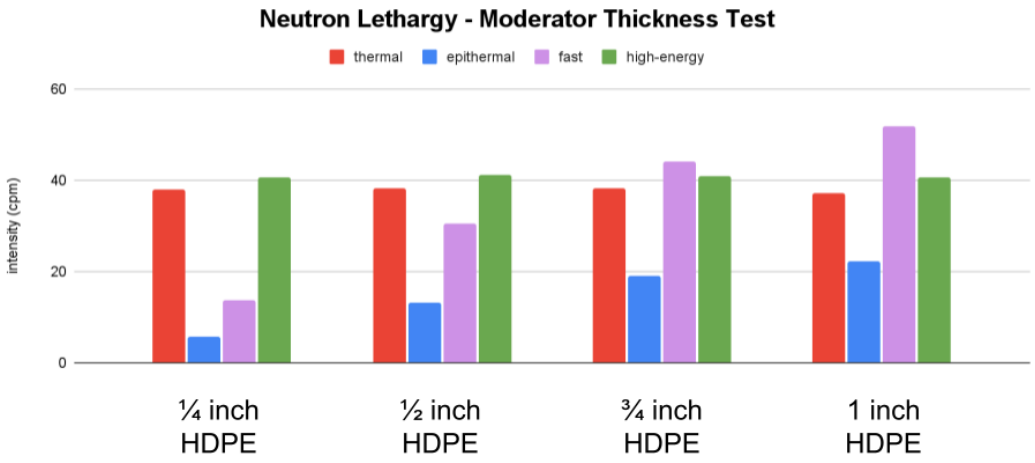

Figure 32. Neutron Lethargy Spectra Per Moderator Thickness. Thermal neutron data was collected for the duration of the test, but it remains relatively constant. Epithermal and fast energy ranges, approximated from the moderated detector counts, increase steadily with each additional layer of moderator. Note that the expected neutron lethargy shape (compared to Figure 2, b-f) is achieved at approximately 3-4 layers (¾ of an inch to one inch) of moderator.

One of the sheets of moderator could be removed from the detector and the calculated WEH will remain within the accepted error range given the short integration time (cpm rather than cph). Considering weight, removal of two layers is preferable, but the lower count rate would become increasingly difficult to work with in areas with a poor GCR flux and the low integration time (cpm).

Considering error and count rates before and after atmospheric corrections are applied, removal of only one layer is advised.

However, increasing the thickness of the moderator will slow down an increasing percentage of neutrons emitted and moderated in the atmosphere. Thus, increasing the thickness of the moderator changes the energy range the detector is sensitive to, and not necessarily in a linear fashion. This increasing moderator thickness relationship is used in

multisphere (or Bonner sphere) tests [Knoll, 2000; Goldhagen et al., 2002]. Since this test is focusing on a volumetrically larger ^{3}He detector than Goldhagen et al., 2002 used with a thinner moderator on the thermal neutron shielded detector(s), the changes in the actual, measured neutron lethargy spectrum were ignored during this test.

CHAPTER 3

CONCLUSIONS

Summary of Results.

It is understandable that some planetary science papers have assumed that PNS is not possible on Earth. The atmosphere does pose a problem, decreasing the amount of GCRs that can reach the surface (requiring a larger instrument with longer integration times), and increasing the elastic scattering of the neutrons once they find their way out of the subsurface (which needs a thicker moderator, and larger epithermal detector footprint), and decreasing the thermal neutron attenuation length (smaller thermal detector footprint). However, GCRs *do* reach the Earth's surface and we *can* measure neutron counts per minute at the surface much like a PNS on the Moon or Mars, with a few instrumentation alterations (see above), as well as incorporate standardized terrestrial hydrology methods to correct for the presence of a neutron-moderating atmosphere.

For our analog PNS instruments, both detectors of the RV units are sensitive to WEH > ~55% filling at least ~15% of the FOV. The RV bare (thermal) and moderated (epithermal) detectors have radii of ~2 m and ~31 m, respectively, in the typical configuration (tripod-mounted horizontal), though further study of the radius of sensitivity of the bare detector using a region with high quantities of neutron absorbers in place of a pool of WEH is recommended. Changing the instrument angle from horizontal to vertical, or increasing the distance from the surface to the detector, will increase the radius of sensitivity. Therefore, continuing to place planetary PNS in the horizontal orientation to maximize the detection of WEH in the immediate vicinity of the instrument is justified.

Earth.

Vegetation produces a diverging trend in the thermal and epithermal count rates (thermal counts decrease and epithermal counts increase), even in desert environments. If conducting tests in regions with vegetation, it would be wise to adjust count rates for stations with vegetation within the FOV via a 10% decrease in the epithermals, and a ~15% increase in the thermals to correct for the diverging trend, this will allow for the determination of the WEH for the subsurface across all traverse points while ignoring neutrons generated and moderated by plants (just as atmospheric corrections remove neutrons emitted and moderated above the ground). While it is well known that the height of the epithermal and thermal neutron zones in the lethargy spectrum relative to each other for each field measurement is crucial to determining the composition of the subsurface, now we have an estimate of the diverging trend produced by organic materials at or near the surface of a rocky world. Vegetation can also be used as a proxy for high concentrations of H, C, and O at the surface or in the topmost layer.

Zreda et al., 2012 summarized that the thermal detector is best for measuring surface WEH, while the epithermal detector is best suited for measuring subsurface WEH. While there is evidence to support that the thermal detector is most sensitive to WEH at the surface than WEH in the subsurface (vegetation sensitivity test), the epithermal data should consider both water in the subsurface and water at the surface (vegetation sensitivity and radial sensitivity tests). The epithermal sensitivity to both surface and subsurface WEH is further supported by the correction factor for snow (SWE) which terrestrial hydrologists apply to the moderated detector data whenever

snow is present within the FOV. Additional tests of the radial sensitivity of the bare (thermal) detector are recommended.

When considering future test configurations or additional research on the thermal detector radial sensitivity, there are two additional methods that should be considered to confirm the radius of sensitivity of the bare (thermal) detector. The first is to replace the large pool of WEH with a material that has a high concentration of neutron absorbers (like an iron-rich basalt). The second is to repeat the same WEH test with longer integration times. Each of the average counts per increment at the lake were collected in 30-minute intervals. Increasing the interval to ~4+ hours would reduce the influence of cars, kayaks, people, and animals moving in the area by averaging out the times with fewer moving objects in the FOV.

It is also recommended that Earth-based studies consider the results of Mars surface and subsurface H_2O ice as a proxy for snow on Earth. Though it may appear slightly different, as most of the H_2O ice on Mars is beneath CO_2-ice, it indicates that the thermal, epithermal, and fast energy ranges are all affected by H_2O as it gets closer and closer to the surface even without an atmosphere, rather than just the thermal as hypothesized by Zreda et al., 2012.

Future work should also consider that the Earth is the only world yet studied with PNS with a magnetic field, which could affect the GCR flux and thus the neutron count rate as well.

The RV Instruments.

The weight of the moderated detector can also be reduced by removing one sheet of HDPE to increase the portability factor while retaining the current integration time (cpm) and the accuracy of the WEH calculations from the RV moderated detector data in future studies.

The RV units are meant as analogs for planetary PNS instruments, so what can we expect during similar tests on other rocky worlds?

Moon and Mars Comparison.

On the Moon and Mars, the thin atmospheres are considered negligible to neutrons (see Neutron Lethargy Spectrum and Atmospheric Correction sections). Without the presence of an atmosphere, the radii of sensitivity of the two detectors in a PNS instrument will likely be roughly the same, much like that of the DAN instrument [Czarnecki et al., 2020, 2023; Hardgrove et al., 2011; Litvak et al., 2014; Mitrofanov et al. 2012; Tate et al., 2018, 2019; Dibb et al., 2024] rather than offset by an entire order of magnitude like the RV detectors (Radial Sensitivity Quantification Test). Which, in turn, will eliminate the problem of the low count rate for the thermal neutrons.

A negligible atmosphere also eliminates the likelihood of finding verdant rocky worlds, but indicators of life could appear similar to those of desert vegetation, or SOC (which is typically corrected for on Earth, as seen in the calibration equation, 7). Vegetation can also be used as a proxy for high concentrations of C, H, and O at the surface, which is far more common in a variety of scenarios.

The composition of both the Moon and Mars is primarily basaltic, indicating that additional testing moving from regions of high basalt content to low basalt content or traverses across regions with varying types of basalt would be an ideal follow up test.

Moon Comparison.

WEH on the Moon is likely to be in a frost or subsurface layer [Gladstone et al., 2012]. Frost at or near the surface may affect both the thermal and epithermal neutron count rates, while subsurface ice will likely show up most clearly in the epithermal neutron count rate. It may be prudent to consider light snow cover as an analog for surface frost. Though, studies of PNS signals from polar ice on Mars may indicate that subsurface water-ice will look a little different to the detectors than water-ice at the surface.

Mars Comparison.

We know there is ice at both poles of Mars (CO_2 above H_2O at both poles), and we know what affect water-ice beneath a layer of CO_2-ice looks like on the neutron lethargy spectrum (thermals increase while epithermal decrease; see Thermal and Epithermal Detector Uses section). This could be used as a proxy for H_2O (and CO_2) frost at the surface or in the subsurface of the Moon, though analog work on Earth comparing Mars polar ice with Earth snow, surface frost, and subsurface permafrost (with and without surface snow) could be beneficial to neutron spectroscopy analog work and terrestrial hydrology in the future. Terrestrial hydrology work with snow has thus far created a SWE correction factor (see Thermal and Epithermal Detector Uses), applied

only to the epithermal detector, but could benefit from considering the sensitivity of the thermal detector to snow as surface WEH, as suggested by Zreda et al., 2012 and Andreasen et al., 2016.

Comparing the catalogs of compositions found on Mars to changes in count rates on Earth could also help explore the uses of mobile detectors on Earth.

Mercury Comparison.

While a study of basaltic compositions would also benefit Mercury PNS data, as would a comparison with other worlds with a negligible atmosphere, Mercury has a darkening agent giving its terrain an unusually low reflectance that could be the result of high concentrations of C creating a graphite-rich crust [Peplowski et al., 2016]. As indicated by the vegetation test and the use of HDPE as a moderator due to its composition that includes both H and C, the presence of C whether in the subsurface or at the surface cannot be ignored. Future tests in regions with high graphite concentrations or other high C regions is recommended.

Venus Comparison.

On Venus, on the other hand, the atmosphere is considerably denser than that of Earth, and likely contains a considerable amount of sulfuric acid (H_2SO_4) cloud cover [Hansen and Hovenier, 1974; Marov et al. 1980; O'Rourke et al., 2023] as well as a 97% CO_2 atmosphere [Marov et al. 1973; O'Rourke et al., 2023]. If one were to suspend a PNS in the atmosphere of Venus, or drop it through the atmosphere on the way to the surface, it is likely that the peak of fast neutrons originating in the atmosphere would shift

to lower energy ranges as the density of the atmosphere increased and would appear as a smaller and smaller peak in the lower energy ranges (due to the lower quantities of GCRs; unless bringing an active neutron source). In other words, following a similar pattern to simply increasing the thickness of (HDPE) moderators around the detectors like the Bonner sphere (also called multisphere) experiments [Knoll, 2000; Goldhagen et al., 2002], which will also increase the count rate, as seen in the Moderator Thickness Test section. In this hypothetical Venus neutron lethargy model, the water sensitive domain may be a better indicator of other moderators, like the H_2SO_4 of the clouds or the CO_2 atmosphere, shifting the WEH to an acid equivalent hydrogen (AEH) or a CO_2 indicator instead. It is also likely that the thermal neutron peak wouldn't be visible unless the detector was placed directly on the surface, and even then, likely only as a small peak compared to the Moon, Mars, and Earth.

Since the atmosphere of Venus is far denser than that of Earth, we would need to employ correction factors for the neutrons generated and moderated above the surface, similar to those used by terrestrial hydrologists here on Earth. Many of the constants derived for atmospheric corrections on Earth originate from ideal gas assumptions for room temperature scenarios. At the surface of Venus, the atmosphere is nearly 100 times the density of Earth's atmosphere, bearing more resemblance to standing on the bottom of the ocean. The Venus surface temperature is also significantly higher than that of Earth, ranging from ~457-474 Celsius, according to Venera 7 [Marov et al. 1973; O'Rourke et al., 2023]. Density correction factors employed on Venus may be similar to those used for the (semi-solid) snow on Earth (SWE) while also retaining some properties of gasses and fluids like Earth's atmosphere.

Perhaps it is worth experimenting with submerging a PNS in water, though it would likely be quite similar to larger amounts of HDPE, and could instead be likened to the thickest quantities of moderator in multisphere experiments [Knoll, 2000; Goldhagen et al., 2002]. Or utilizing the correction factors for the atmosphere to account for half of the FOV of the kayak data, and altering the ideal gas equations and replacing them for ideal liquid situations for the other half of the FOV could also provide a quick analogy for a Venus-like situation. There exists a subsurface neutron depth model (called Z*), which could be of particular interest in the lake data and the Venus atmosphere, as the model does account for bulk density and weight fractions of LW and SOC, though it was designed for Earth atmosphere and surface compositions via MCNP modeling [Franz et al., 2012].

Increased levels of absorbers in granitic and basaltic materials via Earth analogs needs cataloging, as most data thus far has considered only silicic and sedimentary units.

Bringing a neutron source and using an active NS instead of a PNS on Venus is recommended, as the thick atmosphere may prevent GCRs from reaching the surface entirely. Though, as we have learned on Earth, it may not eliminate them entirely. Determining where in the upper atmosphere PNS is no longer feasible could provide insight into a clearer definition of a non-negligible atmosphere for neutron spectroscopy (both passive and active) as well as provide additional insights and clearer definitions of the four energy ranges for the neutron lethargy spectra.

The increased density of the atmosphere might reduce the radius of sensitivity of the thermal detector another order of magnitude or two, reducing the FOV to mere centimeters, which could be useful for determining the composition of thin layers.

Moderator thickness could also create a weight problem, as the thickness of moderators used on Earth is a function of the atmosphere, as well as the gas composition and volume and pressure of the detector itself, if it is needed. Simulations would help determine the specific instrument parameters required for such an endeavor.

Recommendations for Future Studies.

Regardless of the world in question, more data using the RV planetary analog instrument in environments with higher concentrations of neutron moderators (i.e.: hydrated minerals, graphite or high-C content) and absorbers (salts, basalt, granite), as well as an increasing number of shallow layers, and perhaps even submerged in water (to simulate the Venus atmosphere), is recommended.

Confirming the radius of sensitivity of the RV units via a MCNP model, particularly for the bare detector is also recommended.

Additional work on measuring the radius of sensitivity of the bare detector in the field using high quantities of thermal neutron absorbers in place of WEH, and/or repeating the WEH test with longer integration times, are recommended.

If conducting analog field tests in regions with vegetation, it would be wise to adjust count rates via a 10% decrease in the epithermal rates, and a ~15% increase in the thermal rates to correct for the diverging trend in order to determine the WEH for the subsurface and eliminate confusion with regions with changing neutron absorber concentrations.

REFERENCES

American Chem. Council (2024) Chemistry and Automobiles Report https://plasticmakers.org/wp-content/uploads/2023/02/Chemistry-and-Automobiles-2024.pdf

Andreasen, M., K. H. Jensen, M. Zreda, D. Desilets, H. Bogena, and M. C. Looms (2016), Modeling cosmic ray neutron field measurements, Water Resour. Res., 52, 6451–6471, doi:10.1002/2015WR018236.

Andreasen, M., Jensen, K. H., Desilets, D., Franz, T. E., Zreda, M., Bogena, H. R., and Looms, M. C. (2017). Status and perspectives on the cosmic-ray neutron method for soil moisture estimation and other environmental science applications. Vadose Zone J. 16(8). doi:10.2136/vzj2017.04.0086.

Baatz, R., H. R. Bogena, H.-J. Hendricks Franssen, J. A. Huisman, C. Montzka, and H. Vereecken (2015), An empirical vegetation correction for soil water content quantification using cosmic ray probes, Water Resour. Res., 51, 2030–2046, doi:10.1002/2014WR016443.

Bazilevskaya, G. A, Okylophkov, V. P., Charakhchyan, T. N. (1973). Influence of the Interplanetary Magnetic Field Sector on the Galactic Cosmic Ray Modulation. Proceedings of the 13th International Conference on Cosmic Rays, Vol. 2 (MG and SP sessions), p1102.

Berner A.et al. (2022) Measuring Hydration of Nearby Cliffs in Gale Crater Using Neutron Observations. LPSC LIII Abs#2596. https://www.hou.usra.edu/meetings/lpsc2022/pdf/2596.pdf

Berner A.et al. (2023) Analyzing the Effect of High-Relief Topography on Active Neutron Measurements. LPSC LIV Abs#2686. https://www.hou.usra.edu/meetings/lpsc2023/pdf/2686.pdf

Berner A.et al. (2024) Simulating Active Neutron Measurements in Lunar Pits. LPSC LV Abs#2729. https://www.hou.usra.edu/meetings/lpsc2024/pdf/2729.pdf

Bogena, H. R., Huisman, J. A., Baatz, R., Hendricks Franssen, H.-J. and Vereecken, H. (2013) Accuracy of the cosmic-ray soil water content probe in humid forest ecosystems: the worst case scenario. Water Resources Research, vol. 49, no. 9, pp. 5778–5791.

Bolton, D. (1980) the Computation of Equivalent Potential Temperature. Monthly Weather Review Vol. 108 pp. 1046-1053.

Brooks, F. D., and Klein, H. (2002). Neutron Spectrometry - Historical Review and Present Status. Nuclear Instruments and Methods in Physics Research A 476 1-11. DOI:10.1016/S0168-9002(01)01378-X

Byrne, S., and A. P. Ingersoll, Martian climatic events on timescales of centuries: Evidence from feature morphology in the residual south polar ice cap, Geophys. Res. Lett., 30(13), 1696, doi:10.1029/2003GL017597, 2003.

Carr, M. H. (2006) Surface of Mars. Cambridge University Press. ISBN-13: 978-0521872010.

Czarnecki, S., Hardgrove, C., Gasda, P. J., Gabriel, T. S. J., Starr, M., Rice, M. S.et al. (2020). Identification and description of a silicic volcaniclastic layer in Gale crater, Mars, using active neutron interrogation. Journal of Geophysical Research: Planets, 125, e2019JE006180. https://doi.org/10.1029/2019JE006180

Czarnecki, S., Hardgrove, C., Arvidson, R. E., Hughes, M. N., Schmidt, M. E., Henley, T.et al. (2023). Hydration of a clay-rich unit on Mars, comparison of orbital data to rover data. Journal of Geophysical Research: Planets, 128, e2021JE007104. https://doi.org/10.1029/2021JE007104.

Desilets, D., Zreda, M., Prabu, T. (2006). Extended Scaling Factors for In Situ Cosmogenic Nuclides: New Measurements at Low Latitudes. Earth and Planetary Science Letters 246 265-276. doi:10.1016/j.epsl.2006.03.051.

Desilets, D., M. Zreda, and T. P. A. Ferré (2010), Nature's neutron probe: Land surface hydrology at an elusive scale with cosmic rays, Water Resour. Res., 46, W11505, doi:10.1029/2009WR008726.

Desilets, D., and M. Zreda (2013), Footprint diameter for a cosmic-ray soil moisture probe: Theory and Monte Carlo simulations, Water Resour. Res., 49, 3566–3575, doi:10.1002/wrcr.20187.

Desilets, D., (2017). Calibrating a non-invasive cosmic ray soil moisture probe for snow water equivalent, Hydroinnova Technical Document 17-01, doi:10.5281/zenodo.439105.

Dibb, S. D.et al., (2022) Influence of Nearby Topography on Passive Neutron Count Rates From the Dynamic Albedo of Neutrons Instrument On the Mars Science Laboratory Rover. LPSC LIII Abs#2908. https://www.hou.usra.edu/meetings/lpsc2019/pdf/2908.pdf

Dibb, S. D., Hardgrove, C., Lightholder, J., Heffern, L., & Ehresmann, B. (2024).Observed correlation between local topography and passive neutron measurements from the Dynamic Albedo of Neutrons (DAN) instrument on the Mars Science Laboratory (MSL) rover. Earth and Space Science, 11, e2023EA003130. https://doi.org/10.1029/2023EA003130

Donaldson Hanna, K. et al. (2023). Lunar-VISE: An Investigation of the Moon's Non-Mare Silicic Volcanism. Lunar and Planetary Science Conference LIV. https://www.hou.usra.edu/meetings/lpsc2023/pdf/2152.pdf

Elphic, R.C. et al., (2008), Preliminary Results of Hydrogen Prospecting With a Planetary Rover. Lunar and Planetary Science Conference XXXIX. https://www.hou.usra.edu/meetings/lpsc2008/pdf/2400.pdf

Elphic, R.C. et al., (2015), Neutron Spectrometer Prospecting During the Mojave Volatiles Project Analog Field Test. Lunar and Planetary Science Conference XLVI. https://www.hou.usra.edu/meetings/lpsc2015/pdf/2885.pdf

Ennico-Smith, K.et al., (2020). The Volatiles Investigating Polar Exploration Rover Payload. Lunar and Planetary Science Conference LI. https://www.hou.usra.edu/meetings/lpsc2020/pdf/2898.pdf

Farmer, C. B. et al. (1976) Mars: Northern Summer Ice Cap—Water Vapor Observations from Viking 2. Science 194, 1339-1341. DOI:10.1126/science.194.4271.1339

Feldman, W. C.et al., (1998). Fluxes of Fast and Epithermal Neutrons from Lunar Prospector: Evidence for Water Ice at the Lunar Poles. Science 281, 1496. DOI: 10.1126/science.281.5382.1496.

Feldman, W. C. et al., (1999). The Lunar Prospector Gamma-Ray and Neutron Spectrometers. Nuclear Instruments and Methods in Physics Research A 422 562-566. https://doi.org/10.1029/2000JE001444

Feldman, W. C. et al. (2001). Evidence for Water Ice Near the Lunar Poles. JGR: Planets, vol. 106 E10, p. 23231-23251. https://doi.org/10.1029/2000JE001444

Feldman, W. C., Boynton, W. V., Tokar, R. L., Prettyman, T. H., Gasnault, O., Squyres, S. W., Elphic, R. C., Lawrence, D. J., Lawson, S. L., Maurice, S., McKinney, G. W., Moore, K. R., & Reedy, R. C. (2002). Global Distribution of Neutrons from Mars: Results from Mars Odyssey. Science, 297(5578), 75–78. http://www.jstor.org/stable/3077220

Franz, T. E. et al. (2012). Field Validation of a Cosmic-Ray Neutron Sensor Using a Distributed Sensor Network. Vadose Zone Journal. doi:10.2136/vzj2012.0046

Franz, T. E., M. Zreda, R. Rosolem, and P. A. Ferre (2013), A universal calibration function for determination of soil moisture with cosmic-ray neutrons, Hydrology and Earth System Sciences, 17, 453-460. doi:10.5194/hess-17-453-2013.

Franz, T. E., T. Wang, W. Avery, C. Finkenbiner, and L. Brocca (2015), Combined analysis of soil moisture measurements from roving and fixed cosmic ray neutron probes for multiscale real-time monitoring, Geophys. Res. Lett., 42, 3389–3396, doi:10.1002/2015GL063963.

Franz, T. E. et al., (2016) Using Cosmic-Ray Neutron Probes to Monitor Landscape Scale Soil Water Content in Mixed Land Use Agricultural Systems. Applied and Environmental Soil Science. Vol 2016, Article ID 4323742. http://dx.doi.org/10.1155/2016/4323742

Franz, T. et al., (2018) Soil Moisture Mapping with a Portable Cosmic Ray Neutron Sensor. IEA-TECDOC-1845. https://www.researchgate.net/publication/326744502

Gladstone, G. R., et al. (2012), Far-ultraviolet reflectance properties of the Moon's permanently shadowed regions, J. Geophys. Res., 117, E00H04, doi:10.1029/2011JE003913.

Goldhagen, P., M. Reginatto, T. Kniss, J. Wilson, R. Singleterry, I. Jones, and W. V. Steveninck (2002), Measurement of the energy spectrum of cosmic-ray induced neutrons aboard an ER-2 high-altitude airplane, Nucl. Instrum. Methods Phys. Res., Sect. A, 476(12), 42–51, doi:10.1016/S0168-9002(01)01386-9.

Gonzales, N. R., and Hardgrove, C. (2023), Demonstration of Portable Terrestrial Cosmic-ray Neutron Sensors. Lunar and Planetary Science Conference LIV. https://www.hou.usra.edu/meetings/lpsc2023/pdf/2981.pdf

Gonzales, N. R., and Hardgrove, C. (2024a), Adapting Terrestrial Hydrology Methods for Passive Planetary Neutron Spectroscopy Analog Field Experiments. Lunar and Planetary Science Conference LV. https://www.hou.usra.edu/meetings/lpsc2024/pdf/2738.pdf

Gonzales, N. R., and Hardgrove, C. (2024b), Where IS the Water? Spatial and Subsurface Sensitivity of a Portable, Passive Neutron Detection System During Field Tests. Terrestrial Analogs Workshop II. https://www.hou.usra.edu/meetings/terrestrialanalogs2024/pdf/8033.pdf

Hansen, J. E., and Hovenier, J. W. (1974) Interpretation of the polarization of Venus. J Atmos Sci 31:1137–1160. https://doi.org/10.1175/1520-0469(1974)031%3C1137:IOTPOV%3E2.0.CO;2

Hardgrove, C., Moersch, J., Drake, D. (2011) Effects of Geochemical Composition on Neutron Die-Away Measurements: Implications for Mars Science Laboratory's Dynamic Albedo of Neutrons Experiment. Nuclear Instruments and Methods in Physics Research A 659, 442-455. doi:10.1016/j.nima.2011.08.058

Hewitt, J. E.et al., (1976). Ames Collaborative Study of Cosmic Ray Neutrons. NASA TM X-3329. https://ntrs.nasa.gov/citations/19760008919

Hurtado, R.et al., AGU (2023). Investigating Field-Scale Soil Moisture at Upland Watershed and Ephemeral Lake Sites Using Stationary and Roving Cosmic Ray Neutron Sensing. https://agu.confex.com/agu/fm23/meetingapp.cgi/Paper/1325157

Hurtado, R. Y. (2024). Landscape Position Impacts on the Water Balance in the Chihuahuan Desert: Insights from Cosmic-Ray Neutron Sensing at Upland Watershed and Downstream Playa Sites [Master's Thesis, Arizona State University]. ProQuest Dissertations and Theses Global. https://hdl.handle.net/2286/R.2.N.195333

Hydroinnova LLC, Quaesta Instruments, (2013). CRS-1000 User's Guide, Rev 004-1.

iNaturalist (2024) Seek by iNaturalist (Ver 2.16.3) [Mobile app]. App Store. https://apps.apple.com/us/app/seek-by-inaturalist/id1353224144

Iwema, J., Schron, M., Koltermann Da Silva, J., Schweiser De Paiva Lopes, R., Rosoleum, R., (2021), Accuracy and Precision of the Cosmic-Ray neutron Sensor for Soil Moisture Estimation at Humid Environments. Impacts of Observational Uncertainty on Analysis and Modelling of Hydrological Processes. DOI: 10.1002/hyp.14419

Kieffer, H. H et al. (1976), Martian North Pole Summer Temperatures: Dirty Water Ice. Science 194, 1341-1344. DOI:10.1126/science.194.4271.1341

Knoll, G. F. (2000) Radiation Detection and Measurement. 3rd Ed. John Wiley and Sons, Inc. ISBN 0-471-07338-5. https://phyusdb.wordpress.com/wp-content/uploads/2013/03/radiationdetectionandmeasurementbyknoll.pdf

Kohli, M., M. Schron, M. Zreda, U. Schmidt, P. Dietrich, and S. Zacharias (2015), Footprint characteristics revised for field-scale soil moisture monitoring with cosmic ray neutrons, Water Resour. Res., 51, 5772–5790, doi:10.1002/2015WR017169.

Litvak, M. L. et al. (2014). Local variations of bulk hydrogen and chlorine-equivalent neutron absorption content measured at the contact between the Sheepbed and Gillespie Lake units in Yellowknife Bay, Gale Crater, using the DAN instrument onboard Curiosity, J. Geophys. Res. Planets, 119, 1259–1275, doi:10.1002/2013JE004556.

Litvak, M. L.et al. (2020). Mars Neutron Radiation Environment From HEND/Odyssey and DAN/MSL Observations. Planetary and Space Science 184 104866. https://doi.org/10.1016/j.pss.2020.104866

Martin, T.et al. (2024a). S.P. Hopper: In-Situ Exploration of the Shackleton De Gerlache Ridge. Lunar and Planetary Science Conference LV. https://www.hou.usra.edu/meetings/lpsc2024/pdf/1162.pdf

Martin, T.et al. (2024b). S.P. Hopper: In-Situ Exploration of the Shackleton De Gerlache Ridge. Lunar and Planetary Science Conference LV. https://www.hou.usra.edu/meetings/lpsc2024/pdf/2909.pdf

Marov MYA, Avduevsky VS, Kerzhanovich VV, Rozhdestevensky MK, Borodin NF, Ryabov OL (1973) Venera 8: measurements of temperature, pressure and wind velocity on the illuminated side of Venus. J Atmos Sci 30:1210–1214. https://doi.org/10.1175/1520-0469(1973)030<1210:VMOTPA>2.0.CO;2

Marov MYA, Lystsev VE, Lebedev VN, Lukashevich NL, Shari VP (1980) The structure and microphysical properties of the Venus clouds: Venera 9, 10, and 11 data. Icarus 44:608–639. https://doi.org/10.1016/0019-1035(80)90131-1

Mitrofanov, I., Anfimov, D., Kozyrev, A., Litvak, M., Sanin, A., V. Tret'yakov, Krylov, A., Shvetsov, V., Boynton, W., Shinohara, C., Hamara, D., & Saunders, R. S. (2002). Maps of Subsurface Hydrogen from the High Energy Neutron Detector, Mars Odyssey. Science, 297(5578), 78–81. DOI: 10.1126/science.1073616

Mitrofanov, I. G.et al. (2012), Dynamic Albedo of Neutrons (DAN) Experiment Onboard NASA's Mars Science Laboratory. Space Science Review 170:559-582. doi: 10.1007/s11214-012-9924-y.

O'Rourke, J.G., Wilson, C.F., Borrelli, M.E. et al. Venus, the Planet: Introduction to the Evolution of Earth's Sister Planet. Space Sci Rev 219, 10 (2023). https://doi.org/10.1007/s11214-023-00956-0

Parking Requirements: Guidelines, City of Phoenix Planning and Development Department. TRT/DOC/00070 126-542D. Rev 10/20. https://www.phoenix.gov/pddsite/Documents/TRT/dsd_trt_pdf_00070.pdf

Parsons, A. M. (2020) Review of Nuclear Techniques for Planetary Science. Applications of Nuclear Techniques (CRETE19) International Journal of Modern Physics: Conference Science vol. 50 2060004. DOI: 10.1142/S2010194520600046

Peplowski, P., Klima, R., Lawrence, D. *et al.* Remote sensing evidence for an ancient carbon-bearing crust on Mercury. *Nature Geosci* **9**, 273–276 (2016). https://doi.org/10.1038/ngeo2669

Peplowski, P. N.et al. (2023). Calibration of NASA's Neutron Spectrometer System (NSS) for Landed Measurements of Hydrogen Content of the Lunar Surface. Nuclear Inst. and Methods in Physics Research A 1049 168063. https://doi.org/10.1016/j.nima.2023.168063

Prettyman, T. H. (2007) Chapter 41: Remote Chemical Sensing Using Nuclear Spectroscopy, Encyclopedia of the Solar System, 765-786.

Prettyman, T. H.et al. (2012). Elemental Mapping by Dawn Reveals Exogenic H in Vesta's Regolith. Science Mag. vol. 338.

Rasche, D.et al. (2023) A Change in Perspective: Downhole Cosmic-Ray Neutron Sensing for the Estimation of Soil Moisture. Hydrol. Earth Syst. Sci., 27, 3059-3082. https://doi.org/10.5194/hess-27-3059-2023

Rosolem, R., W. J. Shuttleworth, M. Zreda, T. E. Franz, X. Zeng, and S. A. Kurc (2013), The Effect of Atmospheric Water Vapor on the Cosmic-ray Soil Moisture Signal, J. Hydrometeorol. doi:10.1175/JHM-D-12-0120.1.

Schattan, P., G. Baroni, S. E. Oswald, J. Schöber, C. Fey, C. Kormann, M. Huttenlau, and S. Achleitner (2017), Continuous monitoring of snowpack dynamics in alpine terrain by aboveground neutron sensing, Water Resour. Res., 53, 3615–3634, doi:10.1002/2016WR020234.

Schreiner-McGraw, A. P., Vivone, E. R., Mascaro, G., and Franz, T. E. (2016) Closing the Water Balance with Cosmic-ray Soil Moisture Measurements and Assessing Their Relation to Evapotranspiration in Two Semiarid Watersheds. Hydrol. Earth Syst. Sci., 20, 329-345. doi:10.5194/hess-20-329-2016.

Schrön M, Köhli M, Scheiffele L, Iwema J, Bogena HR, Lv L, Martini E, Baroni G, Rosolem R, Weimar J (2017) Improving calibration and validation of cosmic-ray neutron sensors in the light of spatial sensitivity. *Hydrology and Earth System Sciences*, 21(10):5009–5030

Schrön, M., Oswald, S. E., Zacharias, S., Kasner, M., Dietrich, P., & Attinger, S. (2021). Neutrons on rails: Transregional monitoring of soil moisture and snow water equivalent. Geophysical Research Letters, 48, e2021GL093924. https://doi.org/10.1029/2021GL093924.

Schrön, M., Köhli, M., and Zacharias, S. (2023) Signal contribution of distant areas to cosmic-ray neutron sensors – implications for footprint and sensitivity, Hydrol. Earth Syst. Sci., 27, 723–738, https://doi.org/10.5194/hess-27-723-2023.

Serber, R. (1947) Nuclear Reactions at High Energies. Physical Review Vol. 72, Num. 11, 1114. DOI:https://doi.org/10.1103/PhysRev.72.1114

Shen, B.S.P. (1976). Introduction: Spallation Reactions and their Occurrences. In: Shen, B.S.P., Merker, M. (eds) Spallation Nuclear Reactions and their Applications. Astrophysics and Space Science Library, vol 59. Springer, Dordrecht. https://doi.org/10.1007/978-94-010-1511-0_1

Tate, C. G.et al., (2018). Observed Diurnal Variations in Mars Science Laboratory Dynamic Albedo of Neutrons Passive Mode Data. Nuclear Inst. and Methods in Physics Research, A 892, 70-83. https://doi.org/10.1016/j.nima.2018.02.100

Tate, C. G.et al., (2019). Mars Science Laboratory Dynamic Albedo of Neutrons passive mode data and results from sols 753 to 1292: Pahrump Hills to Naukluft Plateau. Icarus 330, 75-90. https://doi.org/10.1016/j.icarus.2019.04.029

Tian, Z.et al., (2016). Soil Water Content Determination with Cosmic-Ray Neutron Sensor: Correcting Aboveground Hydrogen Effects with Thermal/Fast Neutron Ratio. Journal of Hydrology 540, 923-933. http://dx.doi.org/10.1016/j.jhydrol.2016.07.004

Tuttle Keane, J., Tikoo, S. M., Elliot, L. (2021). Endurance: Lunar South Pole-Aitken Basin Traverse and Sample Return Rover. Mission Concept Study Report for the 2023-2032 Planetary Science and Astrobiology Decadal Survey. https://science.nasa.gov/wp-content/uploads/2023/11/endurance-spa-traverse-and-sample-return.pdf

United States Geological Survey (2021). United States Geological Survey 3D Elevation Program 1 meter Digital Elevation Model. Distributed by OpenTopography. https://doi.org/10.5069/G98K778D. Accessed: 2024-11-06

Vather, T, Everson C, Mengistu M, Franz T. (2018) Cosmic ray neutrons provide an innovative technique for estimating intermediate scale soil moisture. S Afr J Sci. 2018;114(7/8), Art. #2017-0422, 9 pages. http://dx.doi.org/10.17159/sajs.2018/20170422

Vather, T., C. S. Everson, and T. E. Franz (2020), The Applicability of the Cosmic Ray Neutron Sensor to Simultaneously Monitor Soil Water Content and Biomass in an Acacia Mearnsii Forest, Hydrology, 7(3), 48.

Vivoni E.R., Pérez-Ruiz E.R., Keller Z.T.et al. (2021) Long-term research catchments to investigate shrub encroachment in the Sonoran and Chihuahuan deserts: Santa Rita and Jornada experimental ranges. Hydrological Processes. 2021;35:e14031. https://doi.org/10.1002/hyp.14031.

Weimar J, Köhli M, Budach C and Schmidt U (2020) Large-Scale Boron-Lined Neutron Detection Systems as a ^{3}He Alternative for Cosmic Ray Neutron Sensing. Front. Water 2:16. doi: 10.3389/frwa.2020.00016

Zreda, M., Desilets, D., T. P. A. Ferre, Scott, R. L. (2008) Measuring soil moisture content non-invasively at intermediate spatial scale using cosmic-ray neutrons. Geophys. Research Letters, v 35, L21402. doi:10.1029/2008GL035655.

Zreda, M., Shuttleworth, W. J., Zeng, X., Zweck, C., Franz, T., Rosolem, R. (2012) COSMOS: the COsmic-ray Soil Moisture Observing System. Hydrol. Earth Syst. Sci., 16, 4079-4099. doi:10.5194/hess-16-4079-2012.